Atmos. Chem. Phys. Discuss., 13, 16775–16830, 2013
www.atmos-chem-phys-discuss.net/13/16775/2013/
doi:10.5194/acpd-13-16775-2013
© Author(s) 2013. CC Attribution 3.0 License.

Atmospheric Chemistry and Physics
Open Access
Discussions

This discussion paper is/has been under review for the journal Atmospheric Chemistry and Physics (ACP). Please refer to the corresponding final paper in ACP if available.

Quantifying the contributions of natural emissions to ozone and total fine PM concentrations in the Northern Hemisphere

A. Zare[1,2,3], J. H. Christensen[2], A. Gross[2,4], P. Irannejad[1], M. Glasius[3], and J. Brandt[2]

[1]Institute of Geophysics, University of Tehran, Iran
[2]Department of Environmental Science, Aarhus University, Denmark
[3]Department of Chemistry and iNANO, Aarhus University, Denmark
[4]AU Herning, Aarhus University, Denmark

Received: 13 May 2013 – Accepted: 30 May 2013 – Published: 21 June 2013

Correspondence to: A. Zare (aza@dmu.dk)

Published by Copernicus Publications on behalf of the European Geosciences Union.

Abstract

Accurate estimates of emissions from natural sources are needed for reliable predictions of ozone and fine particulate matter ($PM_{2.5}$) using air quality models. In this study, the large-scale atmospheric chemistry transport model, DEHM (the Danish Eulerian Hemispheric Model) is further developed, evaluated and applied to study and quantify the contributions of natural emissions of VOCs, NO_x, NH_3, SO_2, CH_4, PM, CO and sea salt to the concentration of ozone and formation of $PM_{2.5}$ for the year 2006. Natural source categories adopted in the recent model are vegetation, lightning, soils, wild animals and oceans. In this study, the model has been further developed to include more biogenic volatile organic compounds (BVOCs) and to implement a scheme for secondary organic aerosol as well as an updated description of sea-salt emissions. Our simulations indicate that at Northern Hemisphere the contribution from natural emissions to the average annual ozone concentrations over land is between 4–30 ppbV. Among the natural emissions, BVOCs are found to be the most significant contributors to ozone formation, enhancing the average ozone concentration by about 11 % over the land areas of the Northern Hemisphere. The relative contribution of all the natural emissions to ozone is found to be highest in the northern part of South America by about 42 %. Similarly, the highest contribution of all the natural sources to total fine particles over land is found to be in South America by about 74 % and sea-salt aerosols demonstrated to play the most important role. However, over the rest of regions in the model domain the largest contribution from the natural sources to $PM_{2.5}$ is due to wildfires. The contribution from natural emissions to the mean $PM_{2.5}$ concentration over the land areas in the model domain is about 34 %.

1 Introduction

The contributions of various anthropogenic sources to air pollution levels have been a key issue in decades for policy development and regulation. In addition to these

cc BY

sources, natural emissions play an important role in determining ambient levels of harmful atmospheric pollutants, especially the tropospheric ozone and particulate matter (PM). In some cases natural emissions are even estimated to far exceed anthropogenic emissions (Olivier et al., 1996; Guenther et al., 1995). Natural sources have also become more important with the ongoing reductions of anthropogenic emissions and will be even more significant in the future in connection with planning of abatement strategies. Furthermore, since emission rates of natural sources often depend strongly on meteorological conditions (e.g., temperature and wind speed); their contributions to air pollution levels are changing in the future with a changing climate (Heald et al., 2008; Jiang et al., 2010; Hedegaard et al., 2008, 2012, 2013). Although efforts have been carried out to investigate and quantify natural emissions, the uncertainties and gaps with regard to these emissions are still quite large (Schultz et al., 2008; Guenther et al., 1995, 2012). For instance, Simpson et al. (1999) reported an uncertainty within a factor of 3–5 associated with estimation of some natural emissions in Europe. Therefore, improvement of our understanding of natural emissions and quantifying their contribution to present and future air pollution levels has been defined as an important field of research in the air pollution modeling community.

In recent years, the relative roles of natural sources in determining air pollution levels have been investigated using various methods; including chemical analysis of particles sampled from the air (Weijers et al., 2011), meteorological satellite measurements (Streets et al., 2009) and atmospheric modeling.

Modeling studies have been conducted to identify the relative contributions of different natural sources with different techniques of tracking or extracting the source contributions. Mueller and Mallard (2011), for instance, determined the specific impacts of lightning and wildfires on ozone concentrations over the United States using the CMAQ (Community Multiscale Air Quality) model. They found wildfire emissions can add more than 50 ppbV to 8 h natural O_3 in the western US and lightning contributes significantly to ozone level in the southeastern US as much as adding 25–30 ppbV to 8 h natural O_3. However, using the same chemistry transport model (CTM), Koo et al. (2010)

ACPD
13, 16775–16830, 2013

CC BY

found annual average of natural background ozone concentrations increase by up to 4 ppbV over the southeastern US due to added NO from lightning. Other modeling studies have also investigated the contribution from other natural sources such as biogenic emissions on O_3 and PM concentrations over Europe and North America (Zare et al., 2012; Sartelet et al., 2012). Curci et al. (2009), for instance, demonstrated that biogenic volatile organic compounds (BVOC) emissions lead to an enhancement of average summer daily ozone maxima over Europe by 2.5 ppbv (5 %).

In general, most modeling studies that have been done to investigate the role of emissions from natural sources are on the local or regional scales (Kaynak et al., 2008; Allen et al., 2012; Bossioli et al., 2012; Delon et al., 2008; Barnaba et al., 2011). More examples are studies on the role of agricultural ammonia emissions on the fine PM ($PM_{2.5}$) formation that have be done on North Carolina (Wu et al., 2008) and North American (Makar et al., 2009).

The primary objective of this modeling study is to quantify and assess the contributions from most natural emissions to ozone and fine particle concentrations particularly on a larger scale (covering more than the Northern Hemisphere). Despite the fact that some previous studies have examined the contribution of natural emissions on the global scale, they have mostly focused on only one of the sources e.g. wildfires (Jaffe and Wigder, 2012), lightning (Stockwell et al., 1999) and soil biogenic NO emission (Steinkamp et al., 2009). In this study, the individual contributions of the different kinds of natural emissions of NMVOC, NO_x, NH_3, SO_2, CH_4, PM, CO, and sea salt to the total air pollution levels have been investigated. In addition, using the same air quality model gives us the ability to assess and compare the relative importance of natural sources with respect to the production of O_3 and fine PM over the model domain, as well as in different parts of the Northern Hemisphere.

In order to carry out a thorough investigation of natural emissions, first, we need to further develop the description of emissions from various sources adopted in the applied long-range chemistry transport model DEHM (the Danish Eulerian Hemispheric Model). Prior to our modifications, DEHM includes natural emissions of nitrogen ox-

CC BY

ides from soil and lightning activities, ammonia from soils, oceans, and wild animals, isoprene (among VOCs) from vegetation, many species from wildfires, and sea salt. Previous evaluations of the DEHM simulations against available measurements, regarding both anthropogenic and some natural sources have shown satisfying results for different chemical species (Brandt et al., 2012; Zare et al., 2012; Solazzo et al., 2012a, b). However, in this study DEHM has been further developed to include more natural emissions of biogenic volatile organic compounds (BVOCs) and a scheme for describing secondary organic aerosols (SOAs). Moreover, the parameterization used for estimating sea-salt generation has been modified to contain additional features. Evaluation of the modeled total fine PM, against observations, is conducted for both the previous and new model versions to assess improvement of the model performance with the updated description of natural emissions.

Brief descriptions of DEHM with focus on the schemes for natural sources are given in the following section. Model simulations and their evaluations with respect to measurements, for the year 2006, are presented and discussed in Sect. 3. In Sect. 4, we assess the contribution of natural emissions to O_3 and fine PM, and the final section highlights concluding remarks and an outlook for future studies.

2 Model description

2.1 The DEHM chemistry-transport model

The air pollution model, DEHM is a 3-D large-scale Eulerian atmospheric chemistry transport model with a horizontal domain covering the Northern Hemisphere and parts of the Southern Hemisphere (Christensen, 1997; Frohn et al., 2002; Brandt et al., 2012). The model is defined on a polar stereographic projection with a resolution of 150 km × 150 km true at 60° N. In the vertical, the model uses a sigma-coordinate system including 29 irregular layers from the surface to 100 hPa. Anthropogenic emissions in DEHM are included from the RCP database (Representative Concentration Path-

ACPD
13, 16775–16830, 2013

ways) with a $0.5^\circ \times 0.5^\circ$ resolution for the whole domain (Lamarque et al., 2010), except over Europe where emissions are based on the EMEP database with a resolution of 50 km × 50 km (Mareckova et al., 2008). Natural emissions are described in more details in the following subsection.

Meteorological data for running the DEHM model are derived from simulations by the mesoscale meteorological model MM5v3.7 (Grell et al., 1995), with initial and boundary conditions provided by NCEP Final Analyses (FNL) data ($1^\circ \times 1^\circ$ spatial and 6 h temporal resolution).

2.2 Natural emissions in the DEHM model

In order to improve DEHM with a more complete description of natural emissions, we have extended the description of natural emissions with simulations of more VOC emissions (monoterpenes) from biogenic sources and subsequently SOA formation from all BVOC precursors. Furthermore, this revised model includes an updated sea-salt parameterization. Methods and databases for natural emissions from the sources, which are already implemented in DEHM, together with those updated, are described in the following.

2.2.1 NO_x from lightning

Emissions of NO_x due to lightning discharges (hereafter LNO_x) in the atmosphere are derived from the Global Emissions Inventory Activity (GEIA) database (http://geiacenter.org/presentData/lightning.html). It presents the monthly and global distributions of LNO_x with a $1^\circ \times 1^\circ$ resolution, which is described by Price et al. (1997). The algorithm estimates LNO_x based on the number of lightning flashes, the intensity of each flash, the lightning type (cloud-to-ground vs. cloud-to-cloud) and the emission factor per flash. The lightning frequencies are calculated using global cloud data from ISCCP (International Satellite Cloud Climatology Project). The global convective cloud data are provided at a 5 km × 5 km spatial and 3 hourly temporal resolution for the pe-

ACPD
13, 16775–16830, 2013

cc BY

riod 1983–1990. The estimated LNO_x inventory in DEHM is based on an 8 yr average of these data. Price et al. (1997) derived the global rate of cloud-to-ground (CG) flashes of 20–30 flashes s^{-1}, while the frequency for intracloud (IC) flashes is given as 50–70 flashes s^{-1}. Mean energy per flash is assumed to be 6.7 GJ for CG flashes and one tenth of this value for IC flashes.

Using estimated NO_x produced per unit energy of 10×10^{16} (molecules NO/J), Price et al. (1997) found that the mean production rate of LNO_x is 12.2 Tg N yr^{-1} over the global. This estimated emission is within the range of 1–20 Tg N yr^{-1} globally reported in other studies (e.g. Schumann and Huntrieser, 2007).

2.2.2 NO_x from soil

Another recognized natural source of tropospheric NO_x, which is included in DEHM, is biogenic soil emissions. The soil emitted NO_x (hereafter SNOx) fluxes are based on an inventory by Yienger and Levy (1995), which is a function of vegetation type, temperature and precipitation. This global empirical model also includes dependence of the emission on fertilizer usage for agricultural soils, pulsing (the emissions burst following the wetting of a dry soil), biomass burning stimulation and canopy recapture of NO_x (fraction of soil emitted NO_x that is deposited within the canopy before it is exported to the atmosphere).

Yienger and Levy (1995) calculated the emissions every 6 h for one year (1990) using temperature and precipitation fields from a general circulation model. The model estimates global annual emissions of 5.5 Tg N above the canopy, which is in reasonable agreement with earlier simulations (Yienger and Levy, 1995). The data set used in DEHM consists of a global $1^{\circ} \times 1^{\circ}$ distribution of monthly nitrogen oxide, which is also made available through the web site of GEIA.

ACPD
13, 16775–16830, 2013

2.2.3 Ammonia from nature

In DEHM, we also use natural as well as anthropogenic emission inventory for ammonia (NH_3) from the GEIA. This data set contains global NH_3emissions of domestic animals, synthetic fertilizers, biomass burning, biofuel combustion, crops, human population, fossil fuel combustion, industry, natural soils, oceans, and wild animals. The last three sources are considered as natural sources of ammonia in the model. All sources are represented globally with a $1^\circ \times 1^\circ$ resolution and monthly time resolution for the year 1990. These emission factors are reviewed from the literature by Bouwman et al. (1997).

The estimated global total NH_3 emission from all sources is $54\,Tg\,N\,yr^{-1}$, in which contributions of the natural sources of soils under natural vegetation and oceans are 4 % and 15 %, respectively. Wild animals are estimated to have a minor contribution to the global NH_3 emission with total value of $0.1\,Tg\,N\,yr^{-1}$.

2.2.4 Wildfires

The released aerosols and trace gases from wildfire in DEHM include BC, OC, SO_2, CO, NO_x, NH_3, CH_4 and non-methane VOCs (ethane, ethene, propane, propene, methanol, acetaldehyde, benzene, toluene, xylene, isoprene, and monoterpenes). Emissions of gases and carbonaceous particles from vegetation fires are taken from the RETRO inventory (REanalysis of the TROpospheric chemical composition over the past 40 yr; Schultz et al., 2007). The database provides the global emissions with $0.5^\circ \times 0.5^\circ$ spatial resolution and monthly time resolution over a long period (from 1960 to 2000). The approach is based on aggregated estimates of total carbon emissions. The emission rate of every compound is given by

$$E(i) = A \times E_{net}(C) \times ER(i,C) \quad (1)$$

where ER is the emission ratio of compound i relative to the total carbon, A is the burned area and E_{net} is the average amount of carbon per unit area. This emission

ACPD
13, 16775–16830, 2013

CC BY

factor and the burned area are dependent on the geographical region and ecosystem type. Interannual variability of emissions in the RETRO is driven only by variations in the burned area.

In RETRO, the Regional fire model (Reg-FIRM) is used to provide estimates of the burned area variability based on the climate data (Venevsky et al., 2002). Schultz et al. (2008) displayed that the geographical distribution and seasonal pattern of fires for the selected year 1997 agree reasonably well with the results obtained by the Global Fire Emission Database (GFEDv2; van der Werf et al., 2006), which is based on satellite data.

2.2.5 Biogenic VOCs (BVOCs)

BVOCs contribute together with nitrogen oxides to change the ozone budget on regional and global scales. Moreover, BVOCs play a key role in the formation of SOAs (Tsigaridis and Kanakidou, 2003), which can appear to be the major constituent of the atmospheric particulate matter over some regions (Mueller and Mallard, 2011). Therefore, estimation of BVOC as the biogenic precursors of air pollutants is significant when aiming at quantifying impacts of the natural emissions on the atmospheric pollution.

BVOCs consist of a wide variety of compounds. Among them, isoprene is the most abundant one (Guenther et al., 1995) and is an important species for the ozone formation (Atkinson, 2000). In this paper, the focus is also on another BVOC class, namely monoterpenes (MTs). MTs are isomers of two isoprene units, i.e. they are very reactive with short atmospheric lifetime, and as well as isoprene can contribute to production of organic particles. Recently, Zare et al. (2012) described an updated version of DEHM including isoprene emissions using MEGAN (Model of Emissions of Gases and Aerosols from Nature; Guenther et al., 2006). MEGAN estimates an ecosystem dependent emission rate of isoprene based on empirical relationships between key drivers (temperature (Q_T) and radiation (Q_{PAR}), leaf area index (Q_{LAI}), foliage age (Q_{age}) and soil moisture (Q_{SM})). The current study uses also PCEEA algorithm of MEGAN to calculate hourly emission rates of MTs. However, the model characterizes the light and

ACPD
13, 16775–16830, 2013

temperature dependence of MTs based on an alternative emissions process. MTs have the ability to be stored in the plant and emitted from these stored pools. However, they are also emitted immediately after production similar to isoprene (Laothawornkitkul et al., 2009). On the canopy scale, there are combinations of both types of mechanisms. Therefore, the MT emission rates (E) in MEGAN are parameterized using light-dependence fraction (LDF):

$$E = E_0 \times Q_{\text{age}} \times Q_T \times Q_{\text{LAI}} \times Q_{\text{SM}} \times [(1 - \text{LDF}) + Q_{\text{PAR}} \times \text{LDF}] \tag{2}$$

in which E_0 is the basal emission normalized to standard conditions. The compound-dependent LDF shows the fraction of MT emissions influenced by variations in light levels. MEGAN calculates emission rates for seven monoterpene compounds (α-pinene, β-pinene, limonene, myrcene, sabinene, delta3-carene and ocimene). The activity factor Q_T accounts for the effect of variations in temperature on MT emissions as described by Guenther et al. (1995):

$$Q_T = B \times \exp(T - T_s) \tag{3}$$

where T_s is a standard temperature and B is a temperature dependent parameter (K^{-1}) with the value of 0.13 for MTs (Sakulyanontvittaya et al., 2008). Other activity factors are parameterized similar to those for isoprene.

2.2.6 Secondary organic aerosols

In this study, the DEHM model has been further developed, by including a module for SOA treatment. We follow the idea of the two-product approach for SOA formation described by Chung and Seinfeld (2002). This partitioning scheme assumes that parent hydrocarbons undergo oxidation via reaction with O_3, OH and NO_3 and form only two semi-volatile gas products. The empirical values of equilibrium gas-particle partitioning coefficients and stoichiometric coefficients together with the oxidation rate for VOCs are given by Chung and Seinfeld (2002) for MTs and by Henze and Seinfeld (2006) for isoprene and Tsigaridis and Kanakidou (2003) for aromatics. The partitioning coefficients

ACPD
13, 16775–16830, 2013

CC BY

are calculated by the Clausius–Clapeyron equation and the enthalpy of vaporization of $42\,kJ\,mol^{-1}$ is used for all products (Chung and Seinfeld, 2002, and Hoyle et al., 2007).

The products of oxidation via OH and O_3 are considered together and oxidation with NO_3 is considered only for MTs and it is assumed to produce only one yield (Griffin et al., 1999). The concentration of the oxidation products in the gas phase (SOG) is calculated based on the partitioning theory (Pankow, 1994):

$$\mathrm{SOG}_{i,j,k} = \mathrm{SOA}_{i,j,k}(K_{i,j,k} \times M_0) \tag{4}$$

where $\mathrm{SOA}_{i,j,k}$ is the aerosol concentration of the k^{th} product from the reaction of hydrocarbon i^{th} and oxidant j^{th} ; $K_{i,j,k}$ is its partitioning coefficient. M_0 consists of both primary organic aerosols (POAs) and SOAs. These are calculated by an iterative approach.

This model has some limitations, e.g. it does not include aging processes and further reactions in the gas and particulate phases. However, we use this approach in our study because the model combines simplicity with the ability to accurately reproduce the laboratory measurements. In this method, POAs are considered as non-volatile, non-reactive and only served as a surface for the condensation of SOAs. Recently, the Volatility-Basis-Set approach (VBS) is introduced for taking into account the volatility of POAs (Robinson et al., 2007; and Donahue et al., 2006). Using VBS in recent modeling studies has increased the amount of SOAs in polluted regions, which shows a good agreement with measurements in megacity environments (Hodzic et al., 2010). Since VBS expands the 2-product model to consider many volatility bins, it is therefore not computationally advantageous for the current assessment study with focus on the background and natural emissions.

2.2.7 Sea salt

Sea-salt aerosol can significantly enhance constituent of particulate matter in coastal areas (Pryor et al., 2007). In air quality models, the generation of sea spray is described

ACPD
13, 16775–16830, 2013

cc BY

with source functions, which parameterize sea-salt production in terms of some variables. Parameters like wind speed, the thermal stability of the atmospheric and ocean surface layer, salinity and sea-water temperature can influence the flux intensity and size distribution of sea spray (de Leeuw et al., 2000).

Currently, production of sea salt, in DEHM, has been modeled only as a function of wind velocity at the height of 10 m (U_{10}). The method is derived based on a simplified parameterization by Monahan et al. (1986), which calculate the production of aerosol (P) by:

$$P = 0.007 \times (U_{10})^{3.14} \tag{5}$$

This parameterization considers the mechanism of bubble bursting for sea-salt aerosol generation. Since the DEHM model, using this module, underestimates measured sodium concentrations, the emission algorithm has been revised to consider a wider range of particles sizes. In the new version, the diameter of dry particles is expanded in the range from 0.02 to 6 µm and two different parameterization schemes are used for calculating sea spray generation in this interval. We use a source function from bubble-mediated presented by Mårtensson et al. (2003) to produce flux estimates of sea salt with dry diameter up to 1.25 µm. Mårtensson et al. (2003) show that the sea spray generation function (F) is not only dependent on the surface wind but also takes into account the variation of whitecap coverage with sea water temperature (T_w) and salinity:

$$F = 3.84 \times 10^{-6} \times U_{10} \times (A_k T_w + B_k) \tag{6}$$

where A_k and B_k parameters show the dependence of sea-salt flux on the aerosol size. In the new version of DEHM, the Monahan et al. (1986) parameterization of sea-salt emission is used for the rest of particles with larger sizes. This second scheme is a source function, which calculates the rate of sea-salt droplet generation (F) of the aerosol radius at 80 % relative humidity (r) by:

$$F = 1.373 \times (U_{10})^{3.14} \times r^{-3} \times (1 + 0.057 r^{1.05}) \times 10^{1.19 \exp(-b2)} \tag{7}$$

Discussion Paper | Discussion Paper | Discussion Paper | Discussion Paper

ACPD
13, 16775–16830, 2013

Quantifying the contributions of natural emissions

A. Zare et al.

CC BY

in which $b = (0.380 - \log(r))/0.650$. The used relationship between the dry and wet (r) radius is based on Gong et al. (1997).

In the next section, DEHM is evaluated for both the previous and new parameterizations to investigate how much the model is improved.

3 Updating natural emissions in DEHM

Before assessing the impact of natural sources on the air quality levels, we have conducted a series of simulations for monoterpenes and SOA formation using the revised version of DEHM. The simulations of these compounds are evaluated against the available measurements in the model domain. Moreover, the model results with the updated sea-salt emissions are evaluated, and performance of the revised model is compared with that of the recent version.

3.1 Simulation of monoterpenes from vegetation

As mentioned, the hourly biogenic concentrations of MTs ($C_{10}H_{16}$) are simulated by integrating MEGAN into the DEHM model. The described MEGAN algorithm estimates emissions of all seven MT classes on the same domain and resolution as in DEHM. The spatial distribution of the annual MT concentrations which is the sum of the seven compounds is shown in Fig. 1. The simulated concentrations are displayed for the year 2006 in the lowest model layer (thickness of around 12 m) over an extended area of the Northern Hemisphere. The highest concentrations with values above 0.6 ppbV are simulated over the tropics. These result from a combination of large biomass densities and markedly warm regional climate. Furthermore, considerable concentrations are found at higher latitudes in the boreal forest areas, which are covered by coniferous (softwood) trees such as pines and firs with high MT emissions.

Figure 2 shows monthly emission rates (Tg month^{-1}) for each MT compound together with the summation. One can see the emissions peak in July which occurs due

ACPD
13, 16775–16830, 2013

CC BY

to strong temperature dependency of MT emissions. The total annual emission of MTs in the studied area is estimated to 88.4 Tg which is consistent with previous studies of e.g. Guenther et al. (1995). This value is lower in compared to isoprene emissions which has a total emission of 592 $\text{Tg}\,\text{yr}^{-1}$ in the same domain (Zare et al., 2012). With respect to individual MTs, α-pinene shows the highest contribution to the total MTs throughout the year, followed by β-pinene and ocimene.

The evaluations of DEHM for simulation of MTs against measurements from four different sites in the US (two sites) and in Europe (two sites) are summarized in Tables 1 and 2. In Table 1 the DEHM model results are validated against the measurement sites of Hyytiälä, in southern Finland (Taipale et al., 2008), Vielsalm in Belgium (Laffineur et al., 2011), and Harvard Forest in Petersham, MA (McKinney et al., 2011). These three measurement sites are located in vegetation and/or forest zones in rural areas. The simulations are carried out in time periods corresponding to the periods of measurements in the individual sites. The fourth monitoring site is located at Thompson Farm in Durham, New Hampshire (43.10° N and 70.99° W) where the measurements were made in open agricultural fields from 2004 to May 2009 (Haase et al., 2011). Table 2 shows the simulations compared with observations for each year covering the entire period at the site. At all the four sites, the atmospheric concentrations of MTs are measured using the technique of proton transfer reaction mass spectrometry (PTR-MS). Since PTR-MS determines only the mass of the product ions, it is impossible to distinguish between different VOCs within the same mass. The signal at 137 m/z is attributed to the total mixing ratio of MT compounds (Laffineur et al., 2011). The performance of DEHM with respect to the MT concentrations is evaluated according to the correlation coefficient and the fractional bias. The model simulations are correlated with corresponding the measurements in the range of 0.34–0.85. These results are highly satisfactory considering the relatively coarse model resolution in this simulation and also difficulty in accurately evaluation of the short lived BVOCs against measurements. Kanakidou et al. (2005) estimated that the uncertainties in global terpene emissions could be as high as a factor of 5. However, comparison of the mean

ACPD
13, 16775–16830, 2013

concentrations between the observed and calculated data in Table 1 indicates that the simulated concentrations are in good agreement with the measurements for these three sites. Table 2 shows that the model underestimates MTs for the monitoring site in Durham. Uncertainties in the emission algorithm, modeling of chemical pathways and meteorological inputs together with experimental uncertainties (McKinney et al., 2011) could result in this discrepancy. Furthermore, the underestimation of MTs at the Durham site could be due to small MT emission factors used in MEGAN for that region. For instance, Sakulyanontvittaya et al. (2008) showed that MT fluxes are lower with MEGAN compared to another Biogenic Emission Inventory System (BEIS3.0) in most regions in North America. However, the underestimation at this site could also be due to stronger local sources, which cannot be captured by the relatively course resolution of the model.

In Fig. 3, we display the temporal variations of the simulated mean daily MT concentrations against observations at the sites during their corresponding measuring periods and years; for the station in Durham, the year 2008 is shown as an example. The modeled mean daily concentrations of MTs in Hyytiälä, Finland, show a high correlation (0.85) and a small fractional bias (−0.08) compared with measurements. However, the model does not capture the high concentration episode at the end of the simulation period.

3.2 Simulation of SOA formation

Figure 4 shows monthly mean concentrations of SOA simulated by DEHM for January and July 2006. The concentrations are higher over the tropical rainforest, in South America, Africa and East Asia, exceeding 1.5 $\mu g\,m^{-3}$ level on both January and July. Southeastern United States and Europe are also demonstrated with relatively high SOA concentrations but only in the summer time. The geographical distribution of SOA reflects the distribution of the precursor emission. Large concentrations of SOA in July are due to larger biogenic emissions resulted from higher temperatures. On the other hand, high tropical large SOA concentrations in January are due to efficient conversion

ACPD
13, 16775–16830, 2013

of oxidized precursors to the aerosol form in wintertime. This is because the SOA condensation is favored at cold temperatures. In the boreal regions in summer, monoterpenes mostly contribute to SOA formation.

Generally, we have estimated the annual total SOA production of 5.8 Tg over the model domain from both anthropogenic and biogenic sources. However, the contribution of anthropogenic sources is negligible. The total global production of SOAs is a very uncertain quantity. A range of about 2 Tg yr^{-1} to 70 Tg yr^{-1} of total global SOA formation is given in previous modeling studies (Hoyle et al., 2007; Tsigaridis and Kanakidou, 2003; Chung and Seinfeld, 2002).

The mean annual concentrations of SOAs and POAs, together with the ratio of SOAs in the total organic carbon are shown in Fig. 5. The highest SOA concentrations are seen in the regions with the highest emissions of precursors. However, the availability of POAs as a surface for condensation of SOAs also plays an important role in the distribution of SOA concentrations. The emissions of primary organic aerosols are considered in DEHM from fossil fuel and biofuel combustion as well as biomass burning sources with a total value of 24.4 Tg C yr^{-1}. Therefore, the POA concentrations are high in relatively polluted regions such as parts of Asia and Europe, and regions with strong wild fires such as Africa's savannah and tropic. We find that the largest contribution of SOAs to the total organic aerosols (OAs) is 8 %, which occurs in South America. Although this contribution is not high considering the annual average, it becomes dominant (above 70 %) over part of the tropics and the southeastern part of the US in the summertime (not shown). This is due to the fact that the highest emissions of BVOCs, as SOA precursors, occur during the summer period. The major fraction of the total OAs over Europe and Asia, however, consists of POA.

In order to evaluate the model performance, spatial and temporal distributions of simulated OA are compared against measurements from the ground-based network of the Interagency Monitoring of Protected Visual Environments (IMPROVE) (http://vista.cira.colostate.edu/improve/). Figure 6 shows that the model reasonably reproduces the observed spatial distribution of OAs over North America with higher val-

ACPD
13, 16775–16830, 2013

cc BY

ues over the eastern part. However, an underestimation of OA concentration is found at a number of sites. The annual mean value for all stations is estimated to be 0.43 $\mu g\,m^{-3}$, which is lower than the observed mean value of 1.02 $\mu g\,m^{-3}$. This discrepancy might be explained by the underestimation of either POAs or precursors of SOAs and/or partitioning between the gas and particle phases. However, as seen in Fig. 7, the model shows high skill in simulating the daily variability with a high correlation coefficient of 0.81, and a good ability to capture most of the observed variations. In general, considering large uncertainties related to simulating SOAs, this comparison concludes that the model perform relatively well in simulating OAs over the US.

Results for the evaluation of OA concentrations in Europe are presented in Table 3. The table summarizes the model performance statistics for some stations from the EMEP network with available data for the year 2006. The results show that the model underestimates OA concentration over Europe, probably due to the underestimation of POAs and/or BVOC emissions in this area. However, some studies indicate that our understanding of SOA forming processes is insufficient. Recent laboratory experiments have suggested the incorporation of additional atmospheric processes such as further oxidation, formation of organosulfates and oligomerization to form more SOAs (Muller et al., 2012; Kristensen et al., 2013; Emanuelsson et al., 2013). As an example, Hall IV and Johnston (2010) estimated that formation of oligomers can contribute as much as 50 % to the non-volatile SOA mass, and Hoyle et al. (2009) demonstrated that the annual mean SOA burden increased about 59 %, when allowing semi-volatile species to partition to sulphate aerosol. The increase is greatest over industrial areas as well as over regions with high emissions of biogenic precursors (Hoyle et al., 2009; Spracklen et al., 2011). This can particularly elucidate the highest discrepancy of simulated OAs compared to measurements for the two background sites in Italy (Table 3). The stations are located close to metropolitan and industrial cities as well as adjacent the area with the large BVOC emissions in Europe (Zare et al., 2012).

ACPD
13, 16775–16830, 2013

CC BY

3.3 Sea-salt simulation

Figure 8 shows the annual mean spatial distribution of sea-spray aerosols from DEHM calculated by a combined source functions based on Mårtensson et al. (2003) and Monahan et al. (1986). Sea-salt emissions peak in the central parts of the major oceans mainly due to the higher wind speeds in winter. However, in summertime higher sea surface temperatures result in increased particle emissions. Despite that sea salt is a dominant aerosol type over the oceans, the particles can be transported inland with onshore winds and significantly affect the air quality in the coastal areas as well. Here sea-salt simulation from the revised DEHM model is evaluated against observations from the coastal sites over Europe. We use the measurements of sodium concentrations provided at 23 stations from the EMEP monitoring network in the year 2006. Sodium is a reliable tracer for sea salt since it is not subject for chemical reactions, contrary to chloride (Dasgupta et al., 2007). Since the sodium mass fraction of sea salt is 0.306 (Seinfeld and Pandis, 2006), total sea salt from observations is calculated as a product of sodium times 3.26. Figure 9a and 9b shows an evaluation of old and new model results, respectively, compared to measurements on a daily basis for the year 2006 as a mean over the EMEP stations. Compared to the model results obtained using the previous version (Fig. 9a), using the revised algorithm for sea salt improves the performance of DEHM considerably (Fig. 9b). The revised version captures most of the sea-salt episodes, and leading to a very small bias. However, using both schemes result in relatively good correlation coefficients between modeled and measured sea-salt concentrations (i.e. 0.78 and 0.80).

Subsequently, we present how much the simulated total $PM_{2.5}$ concentration in Europe from DEHM is improved by including these revised natural emissions and a scheme for SOA formation. Performances of the revised and previous versions of DEHM for total $PM_{2.5}$ are compared against measured data from 22 EMEP sites (Fig. 10). The total particle concentrations in this evaluation are based on emissions from both anthropogenic and natural sources, and consist of black carbon (fresh and

ACPD
13, 16775–16830, 2013

cc BY

aged), organic carbon (primary and secondary), sea salt and secondary inorganic aerosols (SIAs) (SO_4^{-2}, NO_3^-, NH_4NO_3, NH_4HSO_4 and $(NH_4)_2SO_4$). In the revised version with including SOAs and the alternative sea-salt emissions, the total fine particle concentrations are increased. The annual average value slightly increases from 5.8 μg m^{-3} to 6.4 μg m^{-3}. This results in a relatively better agreement with total fine PM observations. However, DEHM still underestimates the total observed aerosol concentrations.

4 Impacts of natural emissions on air pollution levels

To study the contribution of emissions from all the natural sources to ozone and fine PM, we have conducted a sensitivity simulation by turning off all the natural emissions (hereafter No-NE) against a control simulation. The latter simulation considers all emission sources including both anthropogenic and natural source types. Figure 11 shows the annual average ozone concentration for both simulated cases (anthropogenic emissions only or all emission included) for the year 2006, together with their absolute and relative differences. The highest ozone concentrations are depicted at mid-latitudes where high NO_x emissions coincide with high VOCs. However, the highest contribution of the natural emissions to ozone concentrations is found to be in the tropic, with values of greater than 50 %. Additionally, a significant annual average increase up to 25 % of ozone production due to natural emissions is observed in the Southeastern US. The results can be explained by the BVOC emission distributions that show the largest isoprene emissions in the tropic and temperate regions in the Southeastern US throughout the summertime (Zare et al., 2012). On the contrary, lower contributions are observed over the densely populated regions of Beijing and Shanghai in China and New Delhi in India with values between 5–10 %.

Over Europe, the O_3 concentrations are highest in the southern and central parts, especially over the Mediterranean Sea, whereas the contribution from natural emissions enhances the O_3 concentrations by 13–15 % over the Black Sea, as well as over land

CC BY

areas such as Eastern Europe, Greece and Italy. The absolute contribution from natural emission lies between 4–6 ppbV in these areas while the contribution is 2–4 ppbV in the northern and western parts of Europe. Generally, Fig. 11c shows that over the model domain, natural and biogenic emissions can enhance the ozone concentration by up to 30 ppbV, particularly over land.

In the following, we investigate more specifically the contributions of each individual natural source to the ozone production. Figure 12 shows the relative differences between the ozone concentrations from simulations where the emissions from each natural source are excluded, and that obtained from the control simulation. In this study, natural emissions from soil, lightning, vegetation and wildfire are considered to contribute to ozone formation as a result of emitting compounds of VOCs and oxides of nitrogen (NO_x).

NO is emitted from soil microbial processes (nitrification/denitrification) together with NO from other sources, can be oxidized quickly to NO_2. Figure 12a displays the relative contribution of NO_x (= NO + NO_2) from soils (SNO_x) to the tropospheric ozone concentration over the model domain. The highest SNO_x contributions (above 10 %) to O_3 concentration are seen in the tropical regions, which can be explained by the strong dependency of soil emissions to the temperature and ecosystem type (Yienger and Levy, 1995). The largest relative contribution from SNO_x occurs in the rainforest of South America, in the range of 20–30 % (Fig. 12a). The contribution from lightning (LNO_x) is shown in Fig. 12b, which shows that the largest contribution to O_3 concentrations is up to 20 %. NO_x emissions from lightning are identified mostly as a significant contributor to O_3 production in the upper troposphere (Stockwell et al., 1999). Here, its importance with respect to O_3 is investigated in the lowest model layer (thickness around 12 m). Nevertheless, we demonstrate that the contribution from LNO_x to O_3 concentrations is relatively comparable with or even more than SNO_x (e.g. in Southeast Asia). The largest contribution of LNO_x to O_3 concentration is found over South America and Southeast Asia and is in the range of 10 – 20 %. These areas are favorable for more lightning due to high temperatures and convective clouds.

Discussion Paper | Discussion Paper | Discussion Paper | Discussion Paper |

ACPD
13, 16775–16830, 2013

Quantifying the contributions of natural emissions

A. Zare et al.

cc BY

The role of natural NO_x emissions from lightning and soil is not essential for ozone formation in some regions such as the northeastern part of the US and Europe and is limited to only 2 %, as a result of high anthropogenic NO_x emissions in these regions. On the contrary, Fig. 12c shows that the BVOC emissions can significantly contribute to ozone production everywhere over the domain. Removing BVOC emissions reduces O_3 concentrations by 40 % in the tropics, especially in South America, where the largest emissions also have been estimated by the model (Guenther et al., 2006; Zare et al., 2012). In the southeastern part of the United States, the BVOC contributions to annual mean O_3 are found to be between 20 and 30 % and it can be larger throughout the summertime due to temperate forests with high fluxes of isoprene.

Another natural source of VOCs (and other species) is wildfire. Contribution of the total emissions from wildland and agricultural fires to ozone production is presented in Fig. 12d. Although the trace gases of CH_4, NH_3, CO, NO_x and non-methane VOCs (NMVOCs) are emitted from wildfires, NO_x and NMVOCs are the most important O_3 precursors. Although emissions of methane and carbon monoxide are important for the increase in the background levels, they are long-lived species compared to NO_x and NMVOCs. As depicted, large-scale savannah burning in the dry season in Africa can lead to an enhanced ozone concentration of above 20 %. Although a large number of burnings occur throughout the tropical regions, the emissions are highest in Africa due to lower humidity. On the other hand, Jaffe and Wigder (2012) stated that the nitrogen content of fuels released from savannah fires is high, that can enhance the ozone formation. Other spots with relatively high contributions from wildfire can be seen in Siberia, in the south western part of the US, and in the forests in Thailand with values in the range of 5–10 %.

The effects of naturally emitted primary particles, as well as natural and biogenic emissions which can contribute to secondary aerosol formations and thereby to $PM_{2.5}$ are studied in the following. The spatial distribution of total fine particles calculated by the No-NE simulation against the control simulation is shown in Fig. 13, together with the absolute and relative differences. As expected, the aerosols produced due

ACPD
13, 16775–16830, 2013

CC BY

to human activities are dominant in the industrial and populated areas, such as the northeastern part of the US, central Europe and large parts of India (Fig. 13a), and the contribution of natural emissions to the total $PM_{2.5}$ is less than 15 % (Fig. 13d). In East Asia, China, natural sources can contribute to total $PM_{2.5}$ even lower by only up to 5 %. As it is observed in Fig. 13d, in North America, $PM_{2.5}$ is dominated by anthropogenic sources across the East and by natural sources in the West with contributions by up to 70 %. There are similarities between the distributions of natural contributions to $PM_{2.5}$ in the current study and those found by Mueller and Mallard (2011), in this region.

The high contribution from natural sources by more than 70 % over oceans, seen in Fig. 13d, are owing to salt from sea spray, which contributes by up to 7 $\mu g\,m^{-3}$ to the aerosol concentration. Although in the tropics, in Southeast Asia and South America, the contributions also reach to 70 %, the particle production due to natural sources are low in absolute terms with contribution of up to only 1 $\mu g\,m^{-3}$. The investigation of specific natural sources in these regions will be done subsequently. The most striking result to emerge is that in the savannah and tropical forests in Africa, natural sources enhance the fine PM level by more than 11 $\mu g\,m^{-3}$. This is comparable with anthropogenic productions in some industrial regions e.g. in the North East of US.

The impacts on the $PM_{2.5}$ levels from inclusion of NO_x emissions from soil and lightning, natural NH_3, VOC emissions from biogenic and sea salt, together with emissions from wildfire are shown for every single source type in Fig. 14. Overall, wildland and agricultural fires are identified as the most important sources over land, while over oceans sea-salt emissions play the major role, as expected.

The largest increases of $PM_{2.5}$ due to NO emissions are mostly seen over South America, where the contribution of soil is relatively higher than lightning (20–30 % against 10–20 %). Compared to the other natural emissions, the contribution from natural ammonia to the fine PM concentration is low over the model domain (Fig. 14e). This is expected since NH_3 emissions from natural sources are minor compared to other source categories (not shown). Furthermore, the maximum contribution from natural ammonia is found in the tropical savannah and adjoining wildlife parks, while the emissions of sulphur dioxide and nitrogen oxides, required for formation of SIAs, are low in the region. Another side of this issue can be seen in Fig. 14a, where the anthropogenic ammonia emissions are relatively high over North America and West Africa. Natural NO_x with ammonia reacts to form ammonium nitrate aerosols, contributing to the total fine aerosols by 5–10 %.

As already discussed, the tropical regions and the Southeastern US are favorable for a majority of the BVOC emissions, as SOA precursors, and therefore the highest contribution from BVOCs to the total $PM_{2.5}$ takes place in the proximity of these sources (Fig. 14c). In spite that the production of SOAs in the tropical zone of South America, Southeast Asia and Africa are in the same order (in the range of 0.1–0.5 $\mu g\, m^{-3}$ Fig. 5a), the relative contribution is highest in South America (Fig. 14c) due to the low total fine particles shown in Fig. 13b.

Wildfire can enhance the fine particles not only due to emissions of gases like NO_x and NH_3 to produce SIAs, and VOCs to form SOAs, but also because of primary aerosol emissions such as organic carbon and elemental carbon. The primary aerosols play the most important roles with respect to the contribution to the total $PM_{2.5}$ levels. In general, the highest contributions are seen near fires and in downwind areas by more than 40 %. In contrast to Fig. 12d, wildfire emissions, at the higher latitudes, are also estimated to have a high contribution by more than 40 % to $PM_{2.5}$. The total PM concentrations are typically low in the Arctic and therefore the wildfire contribution in Siberia can be large in the Arctic. Another possible explanation for this might be that at higher latitudes, fires burn at lower temperatures which lead to smoldering combustion to be dominant, in contrast to flaming combustion (Lapina et al., 2008). The process of smoldering tends to release larger amounts of NH_3 and lower amounts of NO and (Jaff and Wider, 2012), and eventually leads to lower concentrations of O_3. Moreover, a large value of NO_x emitted by boreal wildfires can rapidly convert to Peroxyacetyl nitrate (PAN) due to lower temperature (Jacob et al., 1992). PAN is an organic compound found in photochemical smog. Moreover, one can expect that the existence of NH_3 besides low temperatures at high latitudes could be favorable for more SIA formation. On the other hand, O_3 production requires both NO_x and NMVOCs. Therefore, higher VOCs (from vegetation) in tropics can make the region more favorable to form ozone, compared to the North, during wildfire events.

The contribution from wildfires to the total atmospheric fine particles in Eastern Europe and Russia is estimated in the range of 10–30 %. This is higher than the contribution of 5–10 % in the western part of Europe. The difference is partly due to the large number of forest and grassland fires happening during summer in Eastern Europe, and crop residue burning, which is a common practice in the regions. The west to east gradients of wildfire contribution, found in the current study, is consistent with that of Barnaba et al. (2011), who estimated the relative contribution of fires to the European aerosol burden using long term satellite-based measurements. Although we estimate the general impact of wildfire to the fine particles level to be 5–10 % in the southern part of Europe, in the Mediterranean region, higher contributions of 10–20 % are seen in the Iberian Peninsula. Adame et al. (2012) found that wildfire events occur in the northwestern part of the Iberian Peninsula, and pollutants could to be transported approximately 1000 km from north to south. Moreover, in Fig. 14d, a relatively remarkable contribution of 30–40 % is seen over Northern Europe (Scandinavian countries) where major biomass burning episodes can take place (Saarikoski et al., 2007).

Figure 14f shows the effect of calculated sea salt on the concentration of fine particulate matter. As expected, and already mentioned, the sea salt is the most significant contributor to $PM_{2.5}$ concentration over the oceans. However, the sea-salt aerosols generated, over oceans, can be driven by wind to the land. This simulation considers the fraction of fine sea-salt particles (with slower gravitational settling) and therefore the aerosols are subject to travel longer distances in the model. Apparently, the concentration of the particulate matter is enhanced at coastal area by at least 10–20 % and in-land by up to 5 %, on average.

Tables 4 and 5 summarize the total contribution from the individual source categories to O_3 and $PM_{2.5}$ levels over land surfaces. The relative contributions are calculated for the domain covering the Northern Hemisphere (the DEHM mother domain) as well as

cc BY

for the six continental regions: North America, northern part of South America, Asia, Europe, Middle East and northern and central part of Africa. Figure 15 displays the extent of these regions in our study.

Overall, BVOCs are found to be the major contributors to the O_3 increases, by 11 % (on the mother domain), and emissions from wildfires enhance $PM_{2.5}$ level by about 25 % and are the dominant natural contributors. The overall results are similar over the individual regions, except for South America where sea-salt aerosols are estimated as the highest natural contributor to the total $PM_{2.5}$ with about 43 %. In the rest of the regions, sea salt is the second most important contributor to fine particles over lands. No similarity among the regions for the second most important natural contributor to ozone is observed. It is seen that wildfire in North America, soil in South America and Middle East, and lightning in Asia.

We already discussed that the role of naturally emitted ammonia in forming $PM_{2.5}$ is not significant (Fig. 14e). Table 5 shows that the contribution of biogenic sources of VOCs to the total value of $PM_{2.5}$ in some of the regions (e.g. Europe and Middle East) is even smaller than that of ammonia.

To sum up, the effects of emissions from all natural sources combined (No-NE simulations) are estimated to be highest in South America, followed by Africa. The relative contributions of natural sources reach to significant amounts of up to 42 % for ozone and up to 77 % for $PM_{2.5}$. These target regions can be identified as areas with less human activities, as well as having ideal environmental conditions for natural and biogenic emissions.

The last columns in Tables 4 and 5 are included as an air pollution modeling exercise. They show that the sum of the relative contributions obtained from every single source (referred to as the Sum in the tables) can be different from the No-NE simulation results. The contribution from all natural emissions to the total fine PM over the model domain is about 36 % when we calculate it as the sum of all the individual contributions (Sum case), while it is estimated to be about 34 % when turning off all the natural emissions simultaneously (No-NE simulations). Similarly, the contributions to the total ozone concentrations are found to be about 22 % and 23 % for the No-NE and Sum cases, respectively. However, in specific areas the differences can be up to 6 %. The expected differences are due to nonlinearity in the processes of atmospheric chemistry. In other words, life cycles of various atmospheric compositions are coupled together. Thus, a perturbation of one species can affect nonlinearly and even significantly to other compositions, which can feedback and modify the perturbation. The discrepancies presented in the tables shows to be different from region to region, because of different atmospheric chemical regimes in each individual region due to different general air pollution levels (Brandt et al., 2013a, b).

5 Conclusions

In this study, we have used the long-range chemical transport model, DEHM, to investigate effects of natural emissions on the concentration levels of ozone and fine particles in the troposphere. The emissions from some natural sources used in the current modeling practice were updated and evaluated. The updated model, which uses a two-product scheme for the SOA simulations, underestimates available organic aerosol observations in Europe. However, compared to the data from US monitoring sites, they show better agreements. The model results for monoterpenes alone show a good agreement with measurements, especially in Europe. The updated sea-salt functions (combination of Mårtensson et al. (2003) and Monahan et al. (1986) source functions) provide larger fine sea-salt concentrations and this shows a significant improvement of model results against available EMEP observations for 2006.

The mean contribution from all natural emissions has been investigated with respect to ozone and $PM_{2.5}$ concentrations and found to be about 22 % and 34 %, respectively, over the model domain. In general, combination of emissions from natural sources of soil, vegetation, lightning and wildfire contribute to the ozone concentrations in the range of 4–30 ppbV and together with ammonia from nature and sea salt to fine particles in the range of 0.1–11 $\mu g\,m^{-3}$ over land. The highest calculated values for both

ACPD
13, 16775–16830, 2013

CC BY

ozone and PM were seen in Africa. However, the relative contributions from natural sources to ozone and PM were largest in South America with contributions of about 42 % and 77 %, respectively.

In conclusion, the major natural contributors to O_3 were found to be BVOCs, over the mother domain. The dominant natural contributors to the $PM_{2.5}$ levels are wildfire emissions over land and sea-salt aerosols over oceans. Moreover, simulations were conducted to specifically assess the contributions from the individual natural source categories in six continental scale regions: North America, northern part of South America, Asia, Europe, Middle East and northern and central part of Africa. The common feature observed over all regions is that the contribution from BVOCs to O_3 formation is the most important amongst the natural emissions. However, considering the total fine PM over land, the wildfire emissions lead to highest enhancement over all regions except South America where sea-salt particles are the major contributor. It is noteworthy that the current study calculates the annual relative contributions from the individual natural emission categories over the land areas in each region. However, investigations in shorter periods and more limited areas can lead to different results.

To sum up, our study clearly indicates that emissions from natural and biogenic sources significantly influence the air pollution levels. In order to derive reliable conclusions, it is needed to document a relatively good agreement between the total simulated ozone and PM concentrations with measurements as well as their precursors. In this study, we have specifically focused on BVOCs, SOAs and sea salt with respect to improving and evaluating the model. Several air pollution studies, which applied DEHM, have presented satisfactory results from the model evaluations for most species such as ozone (Brandt et al., 2012). However, the model, along the line of most chemistry transport models, underestimates the $PM_{2.5}$ concentrations. Model evaluations for the individual compounds demonstrate that the simulated secondary inorganic aerosols and sea salt are in a good agreement with measurements. Limitations of the current model performance for fine particles in Europe can partly be related to missing wind-blown dust from the Sahara desert where the dust aerosols play an important role in

CC BY

the PM concentrations in parts of Southern Europe, Africa and even the Middle East. However, the dust aerosols contribute mainly to the coarse fraction of PM, and a minor part to fine PM. On the other hand, the underestimation of SOA in Europe was about a factor of 2 (Table 3). We may therefore conclude that better estimations of SOA can significantly improve ability of the model to simulate fine PM levels, at least in Europe. Future work, hence, will be devoted to update DEHM with an improved scheme for secondary formed organic aerosols.

Acknowledgement. We express our gratitude to Karl B. Haase (University of New Hampshire), Bernard Heinesch (University of Liège), Taina Ruuskanen (University of Helsinki) and Karena McKinney (Amherst College, MA) for sharing the measurement data of monoterpenes and discussion on the results. We also thank Christopher Hoyle at Institute for Atmospheric and Climate Science, ETH Zurich, regarding his assistance in organic aerosol modeling.

References

Adame, J. A., Hernández-Ceballos, M. A., Bolívar, J. P., and De la Morena, B.: Assessment of an air pollution event in the southwestern Iberian Peninsula, Atmos. Environ., 55, 245–256, 2012.

Allen, D. J., Pickering, K. E., Pinder, R. W., Henderson, B. H., Appel, K. W., and Prados, A.: Impact of lightning-NO on eastern United States photochemistry during the summer of 2006 as determined using the CMAQ model, Atmos. Chem. Phys., 12, 1737–1758, doi:10.5194/acp-12-1737-2012, 2012.

Atkinson, R.: Atmospheric chemistry of VOCs and NO_x, Atmos. Environ., 34, 2063–2101, 2000.

Barnaba, F., Angelini, F., Curci, G., and Gobbi, G. P.: An important fingerprint of wildfires on the European aerosol load, Atmos. Chem. Phys., 11, 10487–10501, doi:10.5194/acp-11-10487-2011, 2011.

Bossioli, E., Tombrou, M., Karali, A., Dandou, A., Paronis, D., and Sofiev, M.: Ozone production from the interaction of wildfire and biogenic emissions: a case study in Russia during spring 2006, Atmos. Chem. Phys., 12, 7931–7953, doi:10.5194/acp-12-7931-2012, 2012.

CC BY

Bouwman, A. F., Lee, D. S., Asman, W. A. H., Dentener, F. J., Vander Hoek, K. W., and Olivier, J. G. J.: A global high-resolution emission inventory for ammonia, Global Biogeochem. Cy., 11, 561–587, 1997.

Brandt, J., Silver, J., Frohn, L., Geels, C., Gross, A., Hansen, A., Hansen, K., Hedegaard, G., Skjøth, C., Villadsen, H., Zare, A., and Christensen, J. H.: An integrated model study for Europe and North America using the Danish Eulerian Hemispheric Model with focus on intercontinental transport of air pollution, Atmos. Environ., 53, 156–176, 2012.

Brandt, J., Silver, J. D., Christensen, J. H., Andersen, M. S., Bønløkke, J. H., Sigsgaard, T., Geels, C., Gross, A., Hansen, A. B., Hansen, K. M., Hedegaard, G. B., Kaas, E., and Frohn, L. M.: Contribution from the ten major emission sectors in Europe and Denmark to the health-cost externalities of air pollution using the EVA model system – an integrated modelling approach, Atmos. Chem. Phys. Discuss., 13, 5871–5922, doi:10.5194/acpd-13-5871-2013, 2013a.

Brandt, J., Silver, J. D., Christensen, J. H., Andersen, M. S., Bønløkke, J. H., Sigsgaard, T., Geels, C., Gross, A., Hansen, A. B., Hansen, K. M., Hedegaard, G. B., Kaas, E., and Frohn, L. M.: Assessment of past, present and future health-cost externalities of air pollution in Europe and the contribution from international ship traffic using the EVA model system, Atmos. Chem. Phys. Discuss., 13, 5923–5959, doi:10.5194/acpd-13-5923-2013, 2013b.

Christensen, J. H.: The Danish Eulerian Hemispheric Model – a three-dimensional air pollution model used for the Arctic, Atmos. Environ., 31, 4169–4191, 1997.

Chung, S. H. and Seinfeld, J. H.: Global distribution and climate forcing of carbonaceous aerosols, J. Geophys. Res., 107, 4407, doi:10.1029/2001JD001397, 2002.

Curci, G., Beekmann, M., Vautard, R., Smiatek, G., Steinbrecher, R., Theloke, J., and Friedrich, R.: Modelling study of the impact of isoprene and terpene biogenic emissions on European ozone levels, Atmos. Environ., 43, 1444–1455, 2009.

Dasgupta, P. K., Campbell, S. W., Al-Horr, R. S., Ullah, S. M. R., Li, J., Amalfitano, C., and Poor, N. D.: Conversion of sea salt aerosol to NaNO3 and the production of HCl: Analysis of temporal behavior of aerosol chloride/nitrate and gaseous HCl/HNO_3 concentrations with AIM, Atmos. Environ., 41, 4242–4257, 2007.

de Leeuw, G., Neele, F. P., Hill, M., Smith, M. H., and Vignati, E.: Production of sea spray aerosol in the surf zone, J. Geophys. Res., 105, 29397–29409, 2000.

Delon, C., Reeves, C. E., Stewart, D. J., Serça, D., Dupont, R., Mari, C., Chaboureau, J.-P., and Tulet, P.: Biogenic nitrogen oxide emissions from soils–impact on NO_x and ozone over

West Africa during AMMA (African Monsoon Multidisciplinary Experiment): modelling study, Atmos. Chem. Phys., 8, 2351–2363, doi:10.5194/acp-8-2351-2008, 2008.
Donahue, N. M., Robinson, A. L., Stanier, C. O., and Pandis, S. N.: Coupled partitioning, dilution, and chemical aging of semivolatile organics, Environ. Sci. Technol., 40, 2635–2643, 2006.
Emanuelsson, E. U., Hallquist, M., Kristensen, K., Glasius, M., Bohn, B., Fuchs, H., Kammer, B., Kiendler-Scharr, A., Nehr, S., Rubach, F., Tillmann, R., Wahner, A., Wu, H.-C., and Mentel, Th. F.: Formation of anthropogenic secondary organic aerosol (SOA) and its influence on biogenic SOA properties, Atmos. Chem. Phys., 13, 2837–2855, doi:10.5194/acp-13-2837-2013, 2013.
Frohn, L. M., Christensen, J. H., and Brandt, J.: Development of a high resolution nested air pollution model – the numerical approach, J. Comput. Phys., 179, 68–94, 2002.
Gong, S. L., Barrie, L. A., and Blanchet, J. P.: Modeling sea-salt aerosols in the atmosphere: 1, Model development, J. Geophys. Res., 102, 3805–3818, 1997.
Grell, G. A., Dudhia, J., and Stauffer, D. R.: A description of the fifth-generation Penn State/NCAR mesoscale model (MM5), NCAR/TN-398 STR, Penn State/NCAR, 1994.
Griffin, R. J., Cocker, D. R., Seinfeld, J. H., and Dabdub, D.: Estimate of global atmospheric organic aerosol from oxidation of biogenic hydrocarbons, Geophys. Res. Lett., 26, 2721–2724, doi:10.1029/1999GL900476, 1999.
Guenther, A., Hewitt, N., Erickson, D., Fall, R., Geron, C., Graedel, T., Harley, P., Klinger, L., Lerdau, M., McKay, W., Pierce, T., Scholes, B., Steinbrecher, R., Tallamraju, R., Taylor, J., and Zimmerman, P.: A global model of natural volatile organic compound emissions, J. Geophys. Res., 100, 8873–8892, 1995.
Guenther, A., Karl, T., Harley, P., Wiedinmyer, C., Palmer, P. I., and Geron, C.: Estimates of global terrestrial isoprene emissions using MEGAN (Model of Emissions of Gases and Aerosols from Nature), Atmos. Chem. Phys., 6, 3181–3210, doi:10.5194/acp-6-3181-2006, 2006.
Haase, K. B., Jordan, C., Mentis, E., Cottrell, L., Mayne, H. R., Talbot, R., and Sive, B. C.: Changes in monoterpene mixing ratios during summer storms in rural New Hampshire (USA), Atmos. Chem. Phys., 11, 11465–11476, doi:10.5194/acp-11-11465-2011, 2011.
Hall IV, W. A. and Johnston, M. V.: Oligomer content of α-pinene secondary organic aerosol, Aerosol Sci. Technol., 45, 37–45, doi:10.1080/02786826.2010.517580, 2011.

CC BY

Heald, C. L., Henze, D. K., Horowitz, L. W., Feddema, J., Lamarque, J. F., Guenther, A., Hess, P. G., Vitt, F., Seinfeld, J. H., Goldstein, A. H., and Fung, I.: Predicted change in global secondary organic aerosol concentrations in response to future climate, emissions, and land use change, J. Geophys. Res.-Atmos., 113, D05211, doi:10.1029/2007jd009092, 2008.

Hedegaard, G. B., Brandt, J., Christensen, J. H., Frohn, L. M., Geels, C., Hansen, K. M., and Stendel, M.: Impacts of climate change on air pollution levels in the Northern Hemisphere with special focus on Europe and the Arctic, Atmos. Chem. Phys., 8, 3337–3367, doi:10.5194/acp-8-3337-2008, 2008.

Hedegaard, G B., Christensen, J. H., Geels, C., Gross, A., May, K. M. H W., Zare, A., and Brandt, J.: Effects of Changed Climate Conditions on Tropospheric Ozone over Three Centuries, Atmos. Climate Sci., 2, 546–561, 2012.

Hedegaard, G. B., Christensen, J. H., and Brandt, J.: The relative importance of impacts from climate change vs. emissions change on air pollution levels in the 21st century, Atmos. Chem. Phys., 13, 3569–3585, doi:10.5194/acp-13-3569-2013, 2013.

Henze, D. K. and Seinfeld, J. H.: Global secondary organic aerosol from isoprene oxidation, Geophys. Res. Lett., 33, L09812, doi:10.1029/2006GL025976, 2006.

Hodzic, A., Jimenez, J. L., Madronich, S., Canagaratna, M. R., DeCarlo, P. F., Kleinman, L., and Fast, J.: Modeling organic aerosols in a megacity: potential contribution of semi-volatile and intermediate volatility primary organic compounds to secondary organic aerosol formation, Atmos. Chem. Phys., 10, 5491–5514, doi:10.5194/acp-10-5491-2010, 2010.

Hoyle, C. R., Berntsen, T., Myhre, G., and Isaksen, I. S. A.: Secondary organic aerosol in the global aerosol – chemical transport model Oslo CTM2, Atmos. Chem. Phys., 7, 5675–5694, doi:10.5194/acp-7-5675-2007, 2007.

Hoyle, C. R., Myhre, G., Berntsen, T. K., and Isaksen, I. S. A.: Anthropogenic influence on SOA and the resulting radiative forcing, Atmos. Chem. Phys., 9, 2715–2728, doi:10.5194/acp-9-2715-2009, 2009.

Jacob, D. J., Wofsy, S. C., Bakwin, P. S., Fan, S. M., Harriss, R. C., Talbot, R. W., Bradshaw, J. D., Sandholm, S. T., Singh, H. B., Browell, E. V., Gregory, G. L., Sachse, G. W., Shipham, M. C., Blake, D. R., and Fitzjarrald, D. R.: Summertime photochemistry of troposphere at high northern latitudes, J. Geophys. Res., 97, 16421–16431, 1992.

Jiang, X., Yang, Z. L., Liao, H., and Wiedinmyer, C.: Sensitivity of biogenic secondary organic aerosols to future climate change at regional scales: an online coupled simulation, Atmos. Environ., 44, 4891–4907, 2010.

ACPD
13, 16775–16830, 2013

Jaffe, D. A. and Wigder, N. L.: Ozone production from wildfires: a critical review, Atmos. Environ., 51, 1–10, doi:10.1016/j.atmosenv.2011.11.063, 2012.
Kanakidou, M., Seinfeld, J. H., Pandis, S. N., Barnes, I., Dentener, F. J., Facchini, M. C., Van Dingenen, R., Ervens, B., Nenes, A., Nielsen, C. J., Swietlicki, E., Putaud, J. P., Balkanski, Y., Fuzzi, S., Horth, J., Moortgat, G. K., Winterhalter, R., Myhre, C. E. L., Tsigaridis, K., Vignati, E., Stephanou, E. G., and Wilson, J.: Organic aerosol and global climate modelling: a review, Atmos. Chem. Phys., 5, 1053–1123, doi:10.5194/acp-5-1053-2005, 2005.
Kaynak, B., Hu, Y., Martin, R. V., Russell, A. G., Choi, Y., and Wang, Y.: The effect of lightning NO_x production on surface ozone in the continental United States, Atmos. Chem. Phys., 8, 5151–5159, doi:10.5194/acp-8-5151-2008, 2008.
Koo, B., Chien, C., Tonnesen, G., Morris, R., Johnson, J., Sakulyanontvittaya, T., Piyachaturawat, P., and Yarwood, G.: Natural emissions for regional modeling of background ozone and particulate matter and impacts on emissions control strategies, Atmos. Environ., 44, 2372–2382, 2011.
Kristensen, K., Enggrob, K. L., King, S. M., Worton, D. R., Platt, S. M., Mortensen, R., Rosenoern, T., Surratt, J. D., Bilde, M., Goldstein, A. H., and Glasius, M.: Formation and occurrence of dimer esters of pinene oxidation products in atmospheric aerosols, Atmos. Chem. Phys., 13, 3763–3776, doi:10.5194/acp-13-3763-2013, 2013.
Laffineur, Q., Aubinet, M., Schoon, N., Amelynck, C., Muller, J. F., Dewulf, J., Van Langenhove, H., Steppe, K., Simpraga, M., and Heinesch, B.: Isoprene and monoterpene emissions from a mixed temperate forest, Atmos. Environ., 45, 3157–3168, 2011.
Lamarque, J.-F., Bond, T. C., Eyring, V., Granier, C., Heil, A., Klimont, Z., Lee, D., Liousse, C., Mieville, A., Owen, B., Schultz, M. G., Shindell, D., Smith, S. J., Stehfest, E., Van Aardenne, J., Cooper, O. R., Kainuma, M., Mahowald, N., McConnell, J. R., Naik, V., Riahi, K., and van Vuuren, D. P.: Historical (1850–2000) gridded anthropogenic and biomass burning emissions of reactive gases and aerosols: methodology and application, Atmos. Chem. Phys., 10, 7017–7039, doi:10.5194/acp-10-7017-2010, 2010.
Laothawornkitkul, J., Taylor, J. E., Paul, N. D., and Hewitt, C. N.: Biogenic volatile organic compounds in the earth system, New Phytol., 183, 27–51, 2009.
Lapina, K., Honrath, R. E., Owen, R. C., Martin, M. V., Hyer, E. J., and Fialho, P.: Late summer changes in burning conditions in the boreal regions and their implications for NO_x and CO emissions from boreal fires, J. Geophys. Res.-Atmos., 113, D11304, 2008.

ACPD
13, 16775–16830, 2013

Quantifying the contributions of natural emissions

A. Zare et al.

CC BY

Mårtensson, E. M., Nilsson, E. D., de Leeuw, G., Cohen, L. H., and Hansson, H. C.: Laboratory simulations and parameterization of the primary marine aerosol production, J. Geophys. Res., 108(D9), 4297, doi:10.1029/2002JD002263, 2003.

Makar, P. A., Moran, M. D., Zheng, Q., Cousineau, S., Sassi, M., Duhamel, A., Besner, M., Davignon, D., Crevier, L.-P., and Bouchet, V. S.: Modelling the impacts of ammonia emissions reductions on North American air quality, Atmos. Chem. Phys., 9, 7183–7212, doi:10.5194/acp-9-7183-2009, 2009.

Mareckova, K., Wankmueller, R., Anderl, M., Muik, B., Poupa, S., and Wieser, M.: Inventory Review 2008: Emission Data Reported under the LRTAP Convention and NEC Directive, Status of Gridded Data, Technical report, EMEP Centre on Emission Inventories and Projections, URL, 2008.

McKinney, K. A., Lee, B. H., Vasta, A., Pho, T. V., and Munger, J. W.: Emissions of isoprenoids and oxygenated biogenic volatile organic compounds from a New England mixed forest, Atmos. Chem. Phys., 11, 4807–4831, doi:10.5194/acp-11-4807-2011, 2011.

Monahan, E. G., Spiel, D. E., and Davidson, K. L.: A model of marine aerosol generation via whitecaps and wave disruption, in: Oceanic Whitecaps, edited by: Monahan, E. and Niocaill, G. M., 167–174, D. Reidel, Norwell, Mass., 1986.

Mueller, S. and Mallard, J.: Contributions of natural emissions to ozone and $PM_{2.5}$ as simulated by the community multiscale air quality (CMAQ) model, Environ. Sci. Technol., 45, 4817–4823, 2011.

Müller, L., Reinnig, M.-C., Naumann, K. H., Saathoff, H., Mentel, T. F., Donahue, N. M., and Hoffmann, T.: Formation of 3-methyl-1,2,3-butanetricarboxylic acid via gas phase oxidation of pinonic acid – a mass spectrometric study of SOA aging, Atmos. Chem. Phys., 12, 1483–1496, doi:10.5194/acp-12-1483-2012, 2012.

Olivier, J. G. J., Bouwman, A. F., van der Maas, C. W. M., Berdowski, J. J. M., Veldt, C., Bloos, J. P. J., Visschedijk, A. J. H., Zandveld, P. Y. J., and Haverlag, J. L.: Description of EDGAR Version 2.0: a set of global emission inventories of greenhouse gases and ozone-depleting substances for all anthropogenic and most natural sources on a per country basis and on $1^{\circ} \times 1^{\circ}$ grid, available at: http://www.pbl.nl/en/publications/1996/Description of EDGAR Version 2 0, RIVM/TNO report, Bilthoven, RIVM report nr. 771060 002, 1996.

Pankow, J. F.: An absorption model of the gas/aerosol partitioning involved in the formation of secondary organic aerosol, Atmos. Environ., 28, 189–193, 1994.

ACPD
13, 16775–16830, 2013

Quantifying the contributions of natural emissions

A. Zare et al.

cc BY

Price, C., Penner, J., and Prather, M.: NO_x from lightning, 1. global distribution based on lightning physics, J. Geophys. Res.-Atmos., 102, 5929–5941, 1997.

Pryor, S. C., Barthelmie, R, J., Schoof, J. T., Binkowski, F. S., Delle Monache, L., and Stull, R.: Modeling the impact of sea-spray on particle concentrations in a coastal city, Sci. Total Environ., 391, 132–142, 2007.

Robinson, A. L., Donahue, N. M., Shrivastava, M. K., Weitkamp, E. A., Sage, A. M., Grieshop, A. P., Lane, T. E., Pierce, J. R., and Pandis, S. N.: Rethinking organic aerosols: semivolatile emissions and photochemical aging, Science, 315, 1259–1262, 2007.

Saarikoski, S., Sillanpaa, M., Sofiev, M., Timonen, H., Saarnio, K., Teinila, K., Karppinen, A., Kukkonen, J., and Hillamo, R.: Chemical composition of aerosols during a major biomass burning episode over northern Europe in spring 2006: experimental and modelling assessments, Atmos. Environ., 41, 3577–3589, 2007.

Sakulyanontvittaya, T., Duhl, T., Wiedinmyer, C., Helmig, D., Matsunaga, S., Potosnak, M., Milford, J., and Guenther, A.: Monoterpene and sesquiterpene emission estimates for the United States, Environ. Sci. Technol., 42, 1623–1629, 2008.

Sartelet, K. N., Couvidat, F., Seigneur, C., and Roustan, Y.: Impact of biogenic emissions on air quality over Europe and North America, Atmos. Environ., 53, 131–141, 2012.

Schultz, M., Backman, L., Balkanski, Y., Bjoerndalsaeter, S., Brand, R., Burrows, J., Dalsoeren, S., de Vasconcelos, M., Grodtmann, B., Hauglustaine, D., Heil, A., Hoelzemann, J., Isaksen, I., Kaurola, J., Knorr, W., Ladstaetter-Weienmayer, A., Mota, B., Oom, D., Pacyna, J., Panasiuk, D., Pereira, J., Pulles, T., Pyle, J., Rast, S., Richter, A., Savage, N., Schnadt, C., Schulz, M., Spessa, A., Staehelin, J., Sundet, J., Szopa, S., Thonicke, K., van het Bolscher, M., van Noije, T., van Velthoven, P., Vik, A., and Wittrock, F.: REanalysis of the TROpospheric chemical composition over the past 40 years (RETRO), a long-term global modeling study of tropospheric chemistry, Final Report, Tech. rep., Max Planck Institute for Meteorology, Hamburg, Germany, 2007.

Schultz, M. G., Heil, A., Hoelzemann, J. J., Spessa, A., Thonicke, K., Goldammer, J. G., Held, A. C., Pereira, J. M. C., and van het Bolscher, M.: Global wildland fire emissions from 1960 to 2000, Global Biogeochem. Cy., 22, GB2002, doi:10.1029/2007GB003031, 2008.

Schumann, U. and Huntrieser, H.: The global lightning-induced nitrogen oxides source, Atmos. Chem. Phys., 7, 3823–3907, doi:10.5194/acp-7-3823-2007, 2007.

Seinfeld, J. H. and Pandis, S. N.: Atmospheric Chemistry and Physics: From Air Pollution to Climate Change, 2nd edition, J. Wiley, New York, 2006.

CC BY

Simpson, D., Winiwarter, W., Borjesson, G., Cinderby, S., Ferreiro, A., Guenther, A., Hewitt, C. N., Janson, R., Khalil, M. A. K., Owen, S., Pierce, T. E., Puxbaum, H., Shearer, M., Skiba, U., Steinbrecher, R., Tarrason, L., and Oquist, M. G.: Inventorying emissions from nature in Europe, J. Geophys. Res., 104, 8113–8152, 1999.

Solazzo, E., Bianconi, R., Vautard, R., Wyat Appel, K., Moran, M. D., Hogrefe, C., Bessagnet, B., Brandt, J., Christensen, J. H., Chemel, C., Coll, I., Denier van der Gon, H., Ferreira, J., Forkel, R., Francis, X. V., Grell, G., Grossi, P., Hansen, A. B., Jericevi, A., Kraljevi, L., Miranda, A. I., Nopmongcol, U., Pirovano, G., Prank, M., Riccio, A., Sartelet, K. N., Schaap, M., Silver, J. D., Sokhi, R. S., Vira, J., Werhahn, J., Wolkem, R., Yarwood, G., Zhang, J., Trivikrama Rao, S., and Galmarini, S.: Model evaluation and ensemble modelling of surface-level ozone in Europe and North America in the context of AQMEII, Atmos. Environ., 53, 60–74, 2012a.

Solazzo, E., Bianconi, R., Pirovano, G., Matthias, V., Vautard, R., Moran, M. D., Appel, K. W., Bessagnet, B., Brandt, J., Christensen, J. H., Chemel, C., Coll, I., Ferreira, J., Forkel, R., Vazhappilly Francis, X., Grell, G., Grossi, P., Hansen, A. B., Miranda, A. I., Nopmongcol, U., Prank, M., Sartelet, K. N., Schaap, M., Silver, J. D., Sokhi, R. S., Vira, J., Werhahn, J., Wolke, R., Yarwood, G., Zhang, J., Rao, S. T., and Galmarini, S.: Operational model evaluation for particulate matter in Europe and North America in the context of AQMEII, Atmos. Environ., 53, 75–92, 2012b.

Spracklen, D. V., Jimenez, J. L., Carslaw, K. S., Worsnop, D. R., Evans, M. J., Mann, G. W., Zhang, Q., Canagaratna, M. R., Allan, J., Coe, H., McFiggans, G., Rap, A., and Forster, P.: Aerosol mass spectrometer constraint on the global secondary organic aerosol budget, Atmos. Chem. Phys., 11, 12109–12136, doi:10.5194/acp-11-12109-2011, 2011.

Steinkamp, J., Ganzeveld, L. N., Wilcke, W., and Lawrence, M. G.: Influence of modelled soil biogenic NO emissions on related trace gases and the atmospheric oxidizing efficiency, Atmos. Chem. Phys., 9, 2663–2677, doi:10.5194/acp-9-2663-2009, 2009.

Stockwell, D. Z., Giannakopoulos, C., Plantevin, P. H., Carver, G. D., Chipperfield, M. P., Law, K. S., Pyle, J. A., Shallcross, D. E., and Wang, K. Y.: Modelling NO_x from lightning and its impact on global chemical fields, Atmos. Environ., 33, 4477–4493, 1999.

Streets, D. G., Yan, F., Chin, M., Diehl, T., Mahowald, N., Schultz, M., Wild, M., Wu, Y., and Yu, C.: Anthropogenic and natural contributions to regional trends in aerosol optical depth, 1980–2006, J. Geophys. Res. Atmos., 114, D00D18, doi:10.1029/2008JD011624, 2009.

Taipale, R., Ruuskanen, T. M., Rinne, J., Kajos, M. K., Hakola, H., Pohja, T., and Kulmala, M.: Technical Note: Quantitative long-term measurements of VOC concentrations by PTR-MS – measurement, calibration, and volume mixing ratio calculation methods, Atmos. Chem. Phys., 8, 6681–6698, doi:10.5194/acp-8-6681-2008, 2008.

Tsigaridis, K. and Kanakidou, M.: Global modelling of secondary organic aerosol in the troposphere: a sensitivity analysis, Atmos. Chem. Phys., 3, 1849–1869, doi:10.5194/acp-3-1849-2003, 2003.

van der Werf, G. R., Randerson, J. T., Giglio, L., Collatz, G. J., Kasibhatla, P. S., and Arellano Jr., A. F.: Interannual variability in global biomass burning emissions from 1997 to 2004, Atmos. Chem. Phys., 6, 3423–3441, doi:10.5194/acp-6-3423-2006, 2006.

Venevsky, S., Thonicke, K. S., Sitch, S., and Cramer, W.: Simulating fire regimes in human-dominated ecosystems: Iberian Peninsula case study, Global Change Biol., 8, 984–998, 2002.

Vestreng, V., Adams, M., and Goodwin, J.: Inventory Review 2004, Emission data reported to CLRTAP and under the NEC directive, EMEP/EEA Joint Review Report, Tech. Rep. EMEP-MSCW Rep. 1/2004, Norw. Meteorol. Inst., Oslo, Norway, 2004.

Weijers, E. P., Schaap, M., Nguyen, L., Matthijsen, J., Denier van der Gon, H. A. C., ten Brink, H. M., and Hoogerbrugge, R.: Anthropogenic and natural constituents in particulate matter in the Netherlands, Atmos. Chem. Phys., 11, 2281–2294, doi:10.5194/acp-11-2281-2011, 2011.

Wiacek, A., Peter, T., and Lohmann, U.: The potential influence of Asian and African mineral dust on ice, mixed-phase and liquid water clouds, Atmos. Chem. Phys., 10, 8649–8667, doi:10.5194/acp-10-8649-2010, 2010.

Wu, S. Y., Hu, J. L., Zhang, Y., and Aneja, V. P.: Modeling atmospheric transport and fate of ammonia in North Carolina – Part II: effect of ammonia emissions on fine particulate matter formation, Atmos. Environ., 42, 3437–3451, 2008.

Yienger, J. J. and Levy, H.: Empirical model of global soil-biogenic NO_x emissions, J. Geophys. Res., 100, 11447–11464, 1995.

Zare, A., Christensen, J. H., Irannejad, P., and Brandt, J.: Evaluation of two isoprene emission models for use in a long-range air pollution model, Atmos. Chem. Phys., 12, 7399–7412, doi:10.5194/acp-12-7399-2012, 2012.

CC BY

Table 1. Comparison of the mean (M) monoterpenes concentrations (ppbV) between observed and calculated data by DEHM, using the MEGAN biogenic model, for the time periods corresponding to the measuring period at the individual sites. The evaluations for the sites in the US and in Europe are performed using statics parameters of the correlation coefficient (Corr.) and the fractional bias (FB). *H* is the height of the station above sea-level.

Location	NO. data	Lat.	Long.	*H* (m)	Measuring period	M-Obs	M-Model	Corr.	FB
Finland/ Hyytiälä	1292	61.51° N	24.17° E	180	2006	0.26	0.23	0.85	−0.08
Belgium/ Vielsalm	2564	50.30° N	5.99° E	450	Mar–Sep 2010	0.09	0.06	0.64	−0.43
Massachusetts/ Petersham	880	42.54° N	72.17° W	340	summer 2005	0.18	0.22	0.34	0.19

ACPD
13, 16775–16830, 2013

CC BY

Table 2. Comparison of the mean (M) monoterpenes concentrations (ppbV) between observed and calculated data by DEHM, using MEGAN biogenic model, for the measuring period 2004–2009. The evaluations for the 6 years individually at Thompson Farm in Durham, New Hampshire (US) (Haase et al., 2011) are performed using statistics of the correlation coefficient (Corr.) and the fractional bias (FB).

Measuring period	NO. data	M-Obs	M-Model	Corr.	FB
2004	721	0.93	0.19	0.57	−1.32
2005	3602	0.88	0.15	0.69	−1.41
2006	5434	0.33	0.1	0.44	−1.09
2007	5110	0.39	0.11	0.71	−1.11
2008	6471	0.37	0.09	0.73	−1.22
2009	4075	0.36	0.10	0.52	−1.12

ACPD
13, 16775–16830, 2013

CC BY

Table 3. Comparison of the mean (M) simulated OA concentrations (µg m^{-3}) with observations in Europe in sites from the EMEP network with available data for the year 2006. The model performances based on two-product approach for SOA formation are evaluated by statistic parameters (correlation coefficient (Corr.) and the fractional bias (FB)).

Country/site	Latitude	Longitude	M_Obs	M_Model	Corr.	FB
Italy/Ispra	45.48° N	8.38° E	8.79	1.27	0.39	−1.49
Italy/Montelibretti	42.06° N	12.38° E	6.16	0.89	0.82	−1.49
Schwitzerland/Payerne	46.48° N	6.57° E	2.68	0.65	0.52	−1.22
Austria/Illmitz	47.46° N	16.46° E	2.31	0.60	0.45	−1.16
Germany/Melpitz	52.31° N	12.55° E	2.07	0.89	0.57	−0.79
Spain/Montseny	41.45° N	2.35° E	1.82	0.84	0.54	−0.73
Norway/Birkenes	58.23° N	8.15° E	1.04	0.41	0.42	−0.86

ACPD
13, 16775–16830, 2013

Table 4. Relative contributions (%) of the natural sources with emissions of (a) SNO_x (NO_x from soils), (b) LNO_x (NO_x from lightning), (c) BVOCs, and (d) wildfire emissions to annual average ozone concentrations in 2006. They are calculated for the DEHM mother domain used in this study (Northern Hemisphere), together with six regions. Mean annual O_3 concentrations (ppbV) averaged over each region (Conc.) are shown for the control case with including all emission sources.

Regions	Conc. (ppbV)	Soils	Lightnings	BVOCs	Wildfires	No-NE	Sum
North America	33.4	1.9	1.9	9.7	2.5	15.9	16.0
South America	22.1	12.7	10	24.4	1.1	42.4	48.2
Asia	35.1	2.6	3.2	10.0	2.6	18.1	18.4
Europe	34.2	2.2	1.4	6.4	2.1	12.3	12.1
Middle East	38.7	3.0	1.5	4.3	1.4	10.1	10.2
Africa	32.0	8.5	3.4	13.6	8.6	33.6	34.1
Northern Hemisphere	32.6	4.8	3.2	11.1	3.9	22.3	23.0

ACPD
13, 16775–16830, 2013

Table 5. Relative contributions (%) of the natural sources to annual average $PM_{2.5}$ concentrations in 2006. The impacts of natural emissions of SNO_x (NO_x from soils), LNO_x (NO_x from lightning), BVOCs, together with emissions from wildfires, natural NH_3, and sea salt on $PM_{2.5}$ level are showed. They are calculated for the DEHM mother domain used in this study (Northern Hemisphere), as well as for the six individual regions. Mean annual $PM_{2.5}$ concentrations ($\mu g\, m^{-3}$) averaged over each region (Conc.) are shown for the control case including all emission sources.

Regions	Conc. ($\mu g\, m^{-3}$)	BVOCs	Wildfire	Soil	Lightning	NH_3 from Nature	Sea salt	No-NE	Sum
North America	3.7	0.7	22.3	1.9	0.9	0.8	8.1	33.1	34.7
South America	1.1	5.6	26.5	3.3	2.6	1.2	42.9	77.3	82.1
Asia	7.1	0.6	13.6	1.6	0.8	0.5	3.7	19.7	20.8
Europe	5.6	0.02	14.6	1.7	0.4	0.6	7.3	23.7	24.6
Middle East	5.8	0.00	9.0	1.8	0.5	0.3	6.7	17.4	18.3
Africa	3.9	2.4	60.3	2.3	1.1	0.8	4.5	69.0	71.4
Northern Hemisphere	4.7	1.0	25.2	1.9	0.9	0.6	6.5	34.3	36.1

ACPD
13, 16775–16830, 2013

A. Zare et al.

CC BY

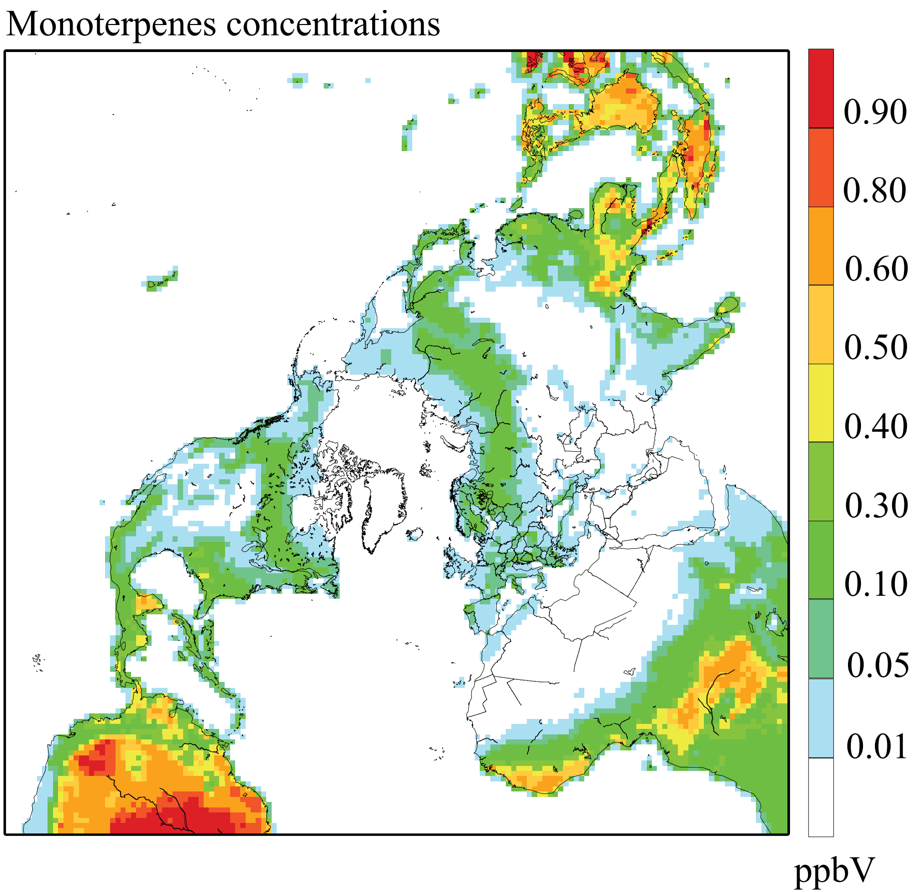

Fig. 1. Spatial distribution of the annual average monoterpenes concentrations (ppbV) simulated by DEHM in the lowest model layer using the MEGAN biogenic emission model for 2006.

ACPD
13, 16775–16830, 2013

cc BY

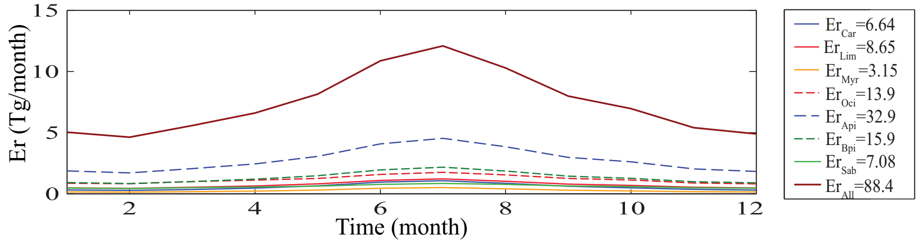

Fig. 2. Monthly emission rates (Tg month^{-1}) for seven monoterpene compounds (α-pinene, β-pinene, limonene, myrcene, sabinene, delta3-carene and ocimene), together with the summation (All) calculated by MEGAN, in a domain covering the Northern Hemisphere, for 2006. Annual fluxes (Tg) of each compound are also given.

ACPD
13, 16775–16830, 2013

Quantifying the contributions of natural emissions

A. Zare et al.

CC BY

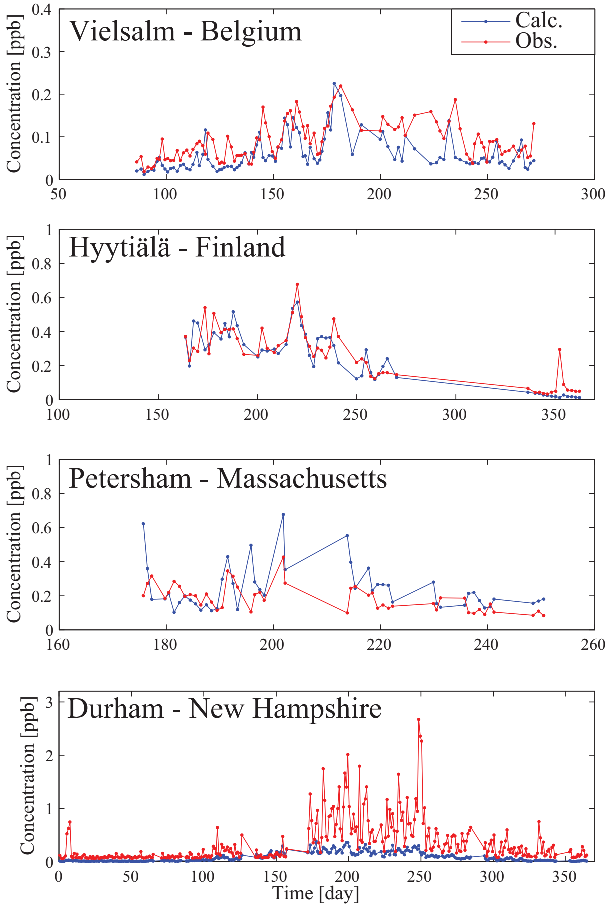

Fig. 3. Validation of the DEHM model results of daily average monoterpene concentrations against measurements from the sites in Belgium, Finland, Massachusetts and New Hampshire for the years 2010, 2006, 2005 and 2008 respectively.

ACPD
13, 16775–16830, 2013

CC BY

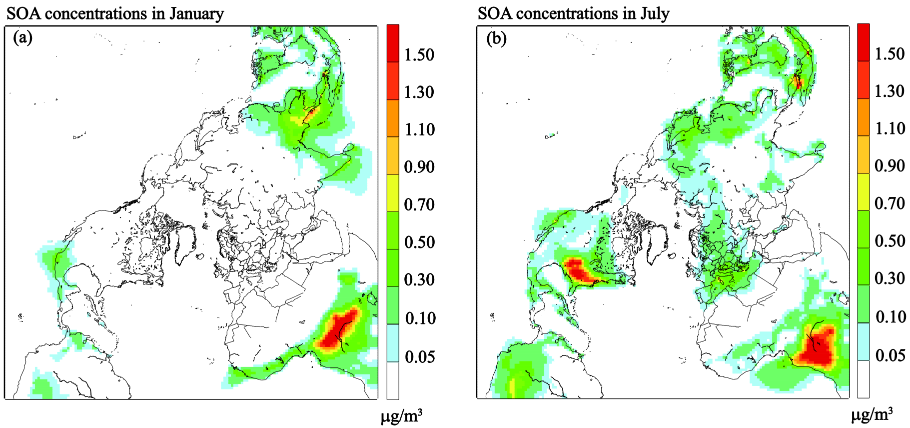

Fig. 4. The surface-layer concentrations ($\mu g\,m^{-3}$) of SOAs in January and July simulated by DEHM based on two-product approach for SOA formation in 2006.

ACPD
13, 16775–16830, 2013

Title Page
Abstract
Introduction
Conclusions
References
Tables
Figures
Back
Close
Full Screen / Esc
Printer-friendly Version
Interactive Discussion

cc BY

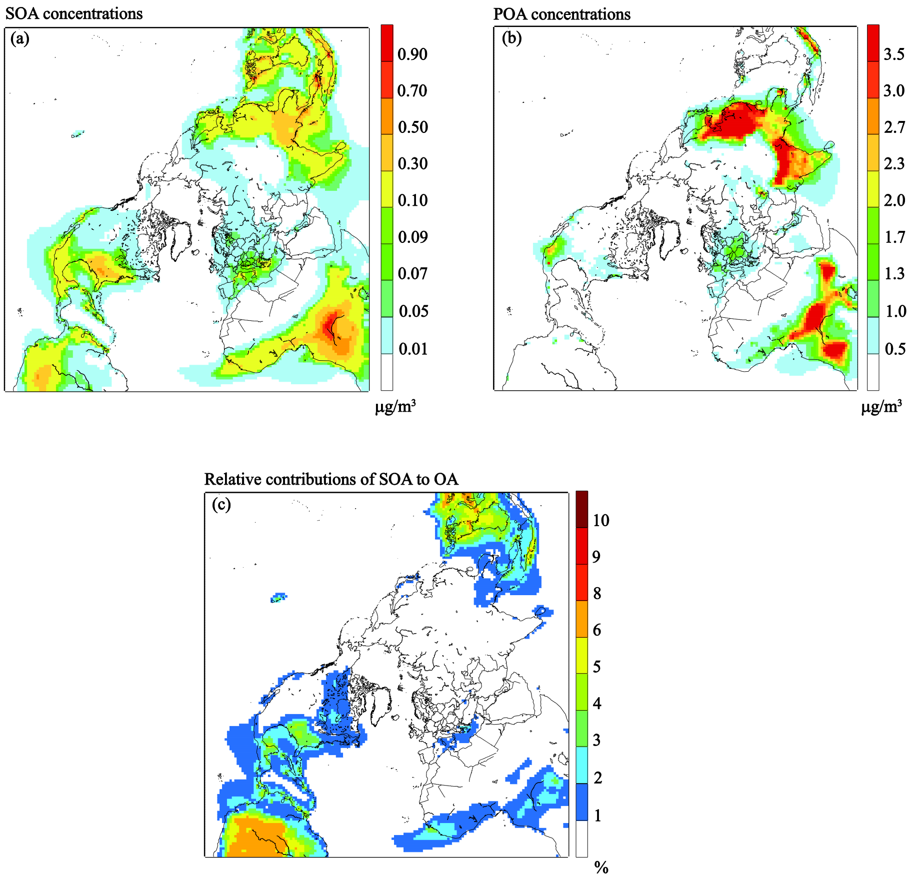

Fig. 5. Geographical distributions of annual average **(a)** SOA and **(b)** POA concentrations ($\mu g\,m^{-3}$) simulated by DEHM for the year 2006. Panel **(c)** shows the ratios of SOAs to total OAs (POAs + SOAs).

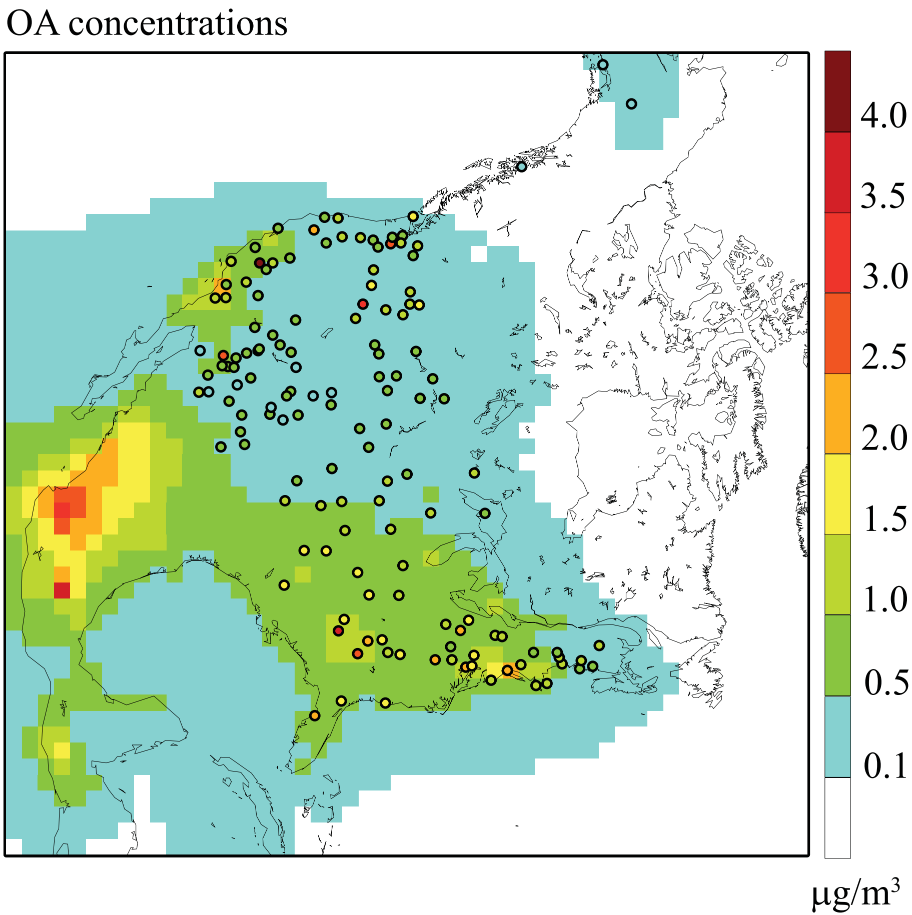

Fig. 6. Spatial distribution of simulated annual average concentration (µg m^{-3}) of OAs (primary and secondary OAs) against measurements (circles) from sites in the IMPROVE network, for 2006.

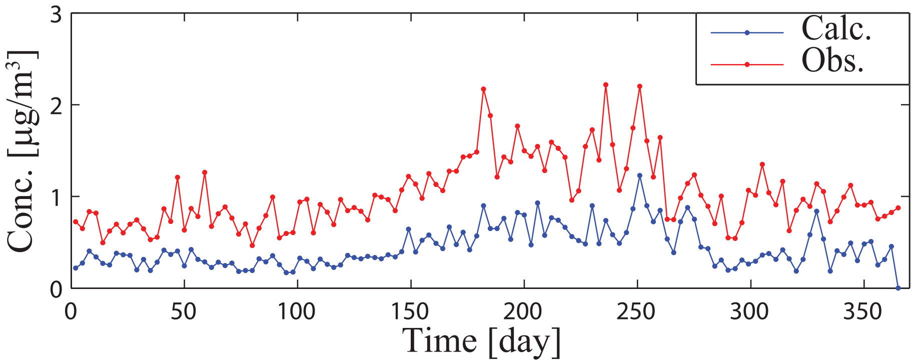

Fig. 7. Daily mean values of the simulated OA concentrations against observations from the IMPROVE network, taken as an average over the sites shown in Fig. 6

ACPD
13, 16775–16830, 2013

Title Page
Abstract | Introduction
Conclusions | References
Tables | Figures
◀| |▶
◀ ▶
Back | Close
Full Screen / Esc
Printer-friendly Version
Interactive Discussion

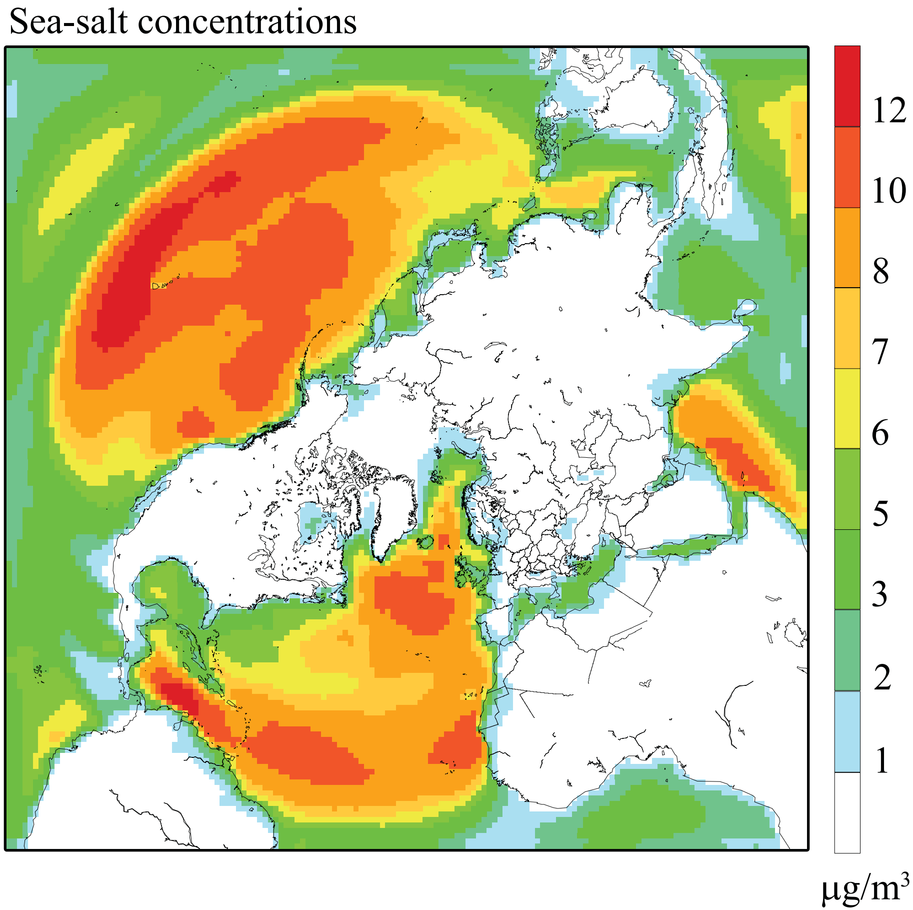

Fig. 8. Annual mean concentrations ($\mu g\,m^{-3}$) of sea salt in 2006 calculated by DEHM using combined source functions based on Mårtensson et al. (2003) and Monahan et al. (1986).

ACPD
13, 16775–16830, 2013

Quantifying the contributions of natural emissions

A. Zare et al.

CC BY

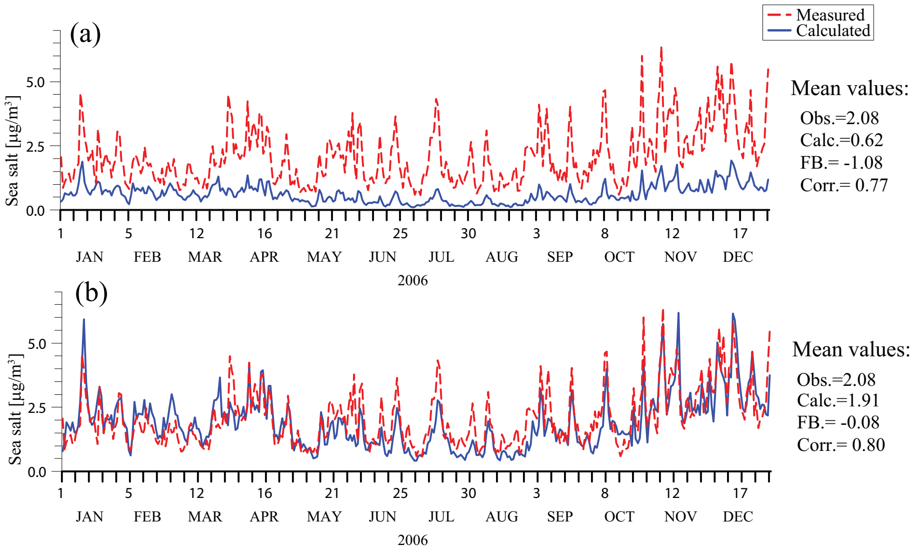

Fig. 9. Evaluation of the sea-salt simulations from DEHM based on **(a)** a simplified parameterization by Monahan et al. (1986), and **(b)** a combined source functions based on Mårtensson et al. (2003) and Monahan et al. (1986) against observations from the EMEP monitoring network in the year 2006.

ACPD
13, 16775–16830, 2013

CC BY

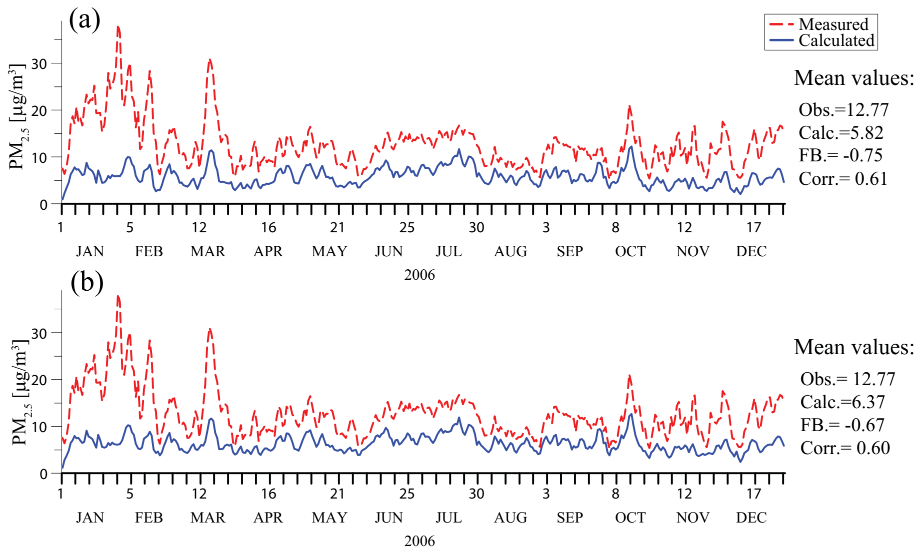

Fig. 10. Evaluation of the simulated total $PM_{2.5}$ concentrations ($\mu g\,m^{-3}$) from **(a)** the recent, and **(b)** the revised versions of DEHM against measured data from the EMEP network. The revised version includes SOA concentrations, as well as using the alternative sea-salt emissions. Total $PM_{2.5}$ in DEHM includes black carbon, organic carbon (primary and secondary), sea salt and secondary inorganic aerosol.

ACPD
13, 16775–16830, 2013

CC BY

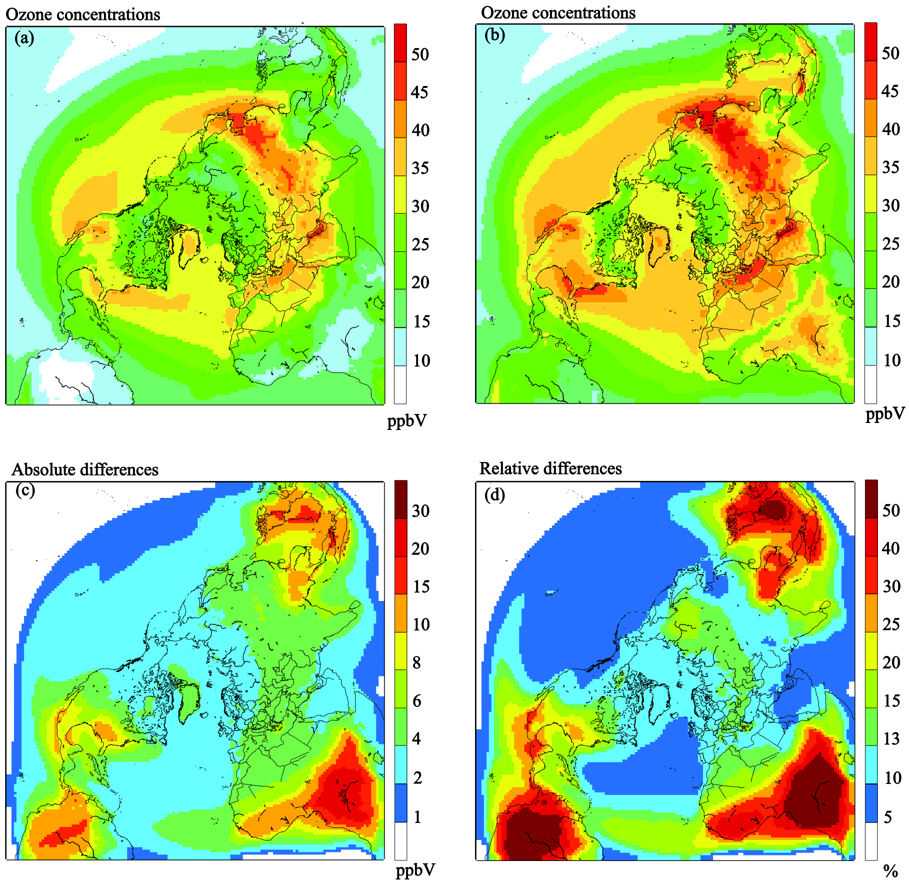

Fig. 11. The annual average ozone concentrations (ppbV) simulated by DEHM for **(a)** a sensitivity simulation by turning off all natural emissions (No-NE), and **(b)** a control simulation including all emission sources, for 2006, together with **(c)** their absolute, **(d)** and relative differences.

CC BY

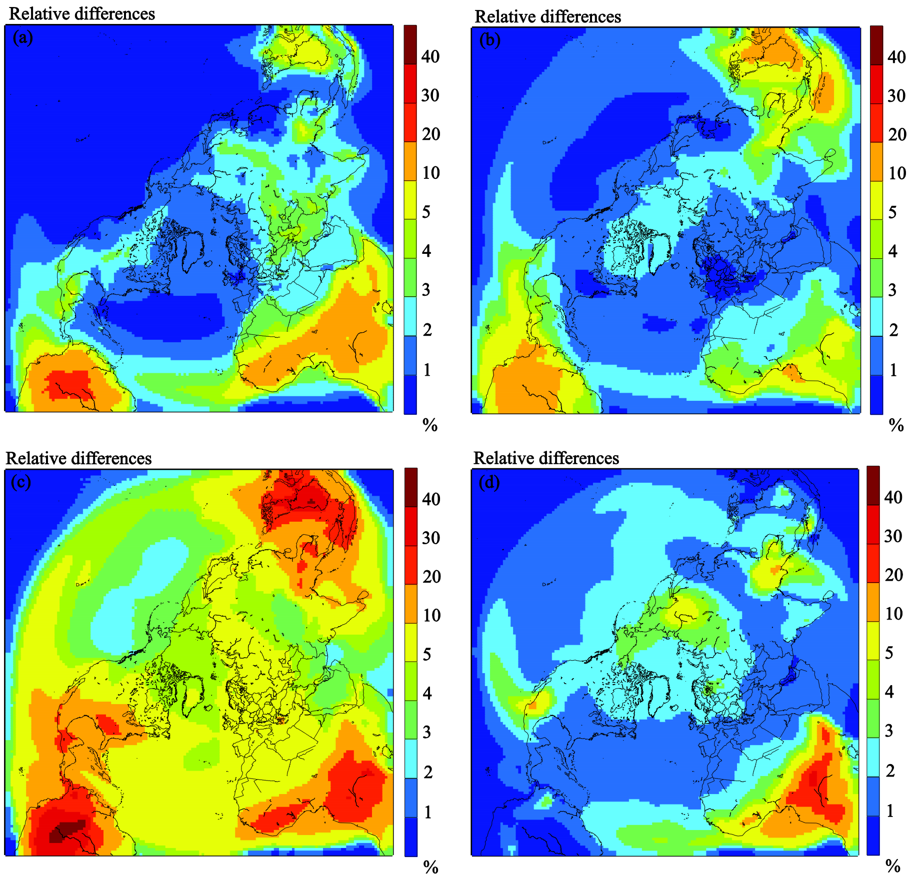

Fig. 12. Relative contributions (%) of the natural sources with emissions of **(a)** SNO_x (NO_x from soils), **(b)** LNO_x (NO_x from lightning), **(c)** biogenic VOCs, and **(d)** wildfire emissions to annual average ozone concentrations in 2006.

CC BY

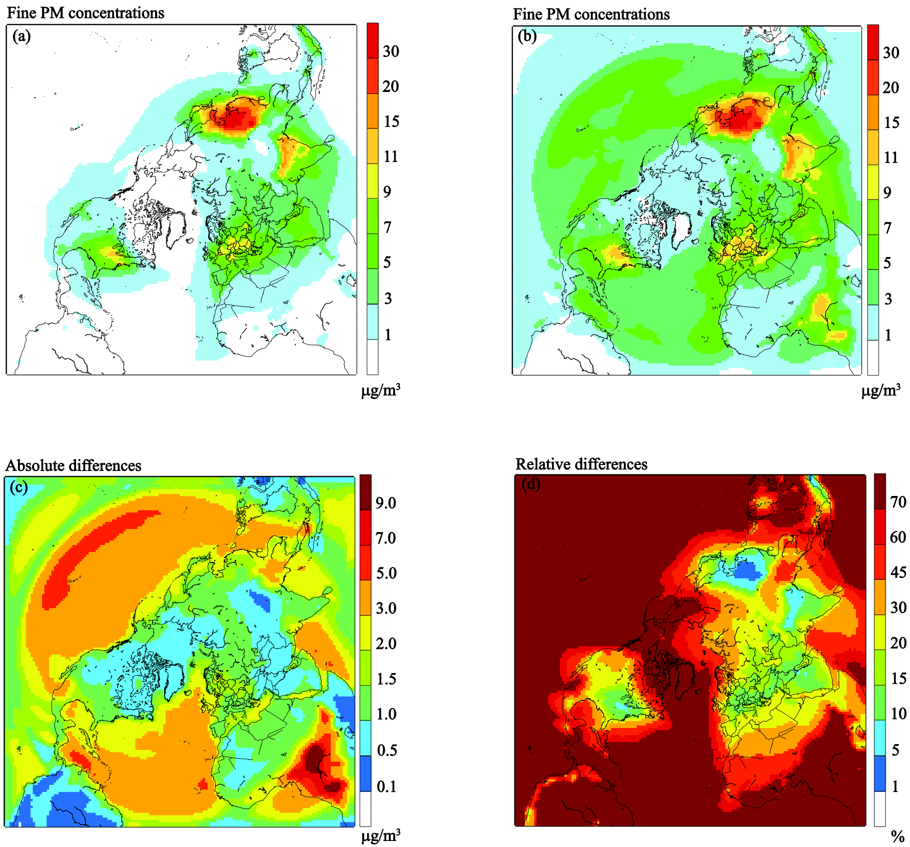

Fig. 13. The annual average $PM_{2.5}$ concentrations ($\mu g\,m^{-3}$) simulated by DEHM for **(a)** a sensitivity simulation by turning off all natural emissions (No-NE), and **(b)** a control simulation including all emission sources, for 2006, together with **(c)** their absolute, **(d)** and relative differences.

ACPD
13, 16775–16830, 2013

Quantifying the contributions of natural emissions

A. Zare et al.

CC BY

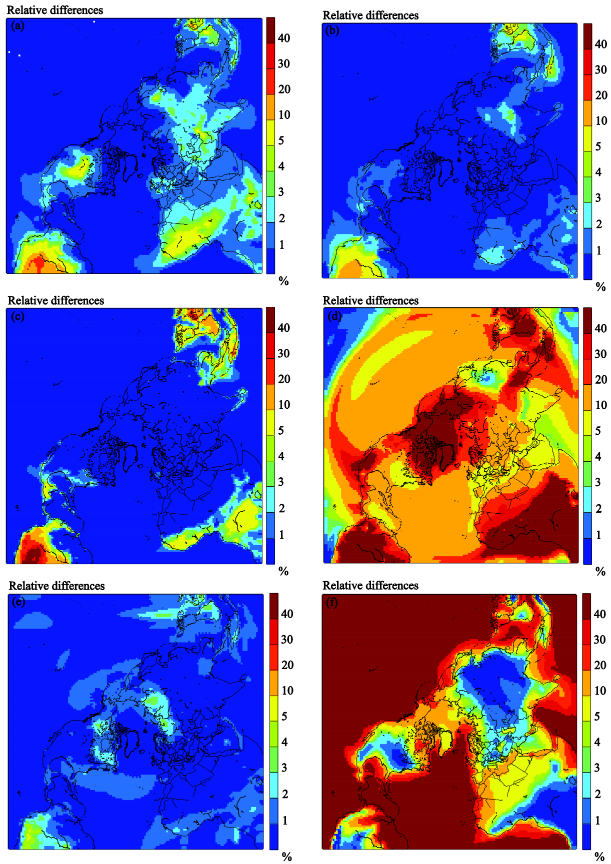

Fig. 14. Relative contributions (%) of the natural sources to annual average $PM_{2.5}$ concentrations in 2006. The impacts of natural emissions of **(a)** SNO_x (NO_x from soils), **(b)** LNO_x (NO_x from lightning), **(c)** biogenic VOCs, emissions **(d)** from wildfires, **(f)** natural NH_3, and **(e)** sea salt on $PM_{2.5}$ levels are shown.

ACPD
13, 16775–16830, 2013

CC BY

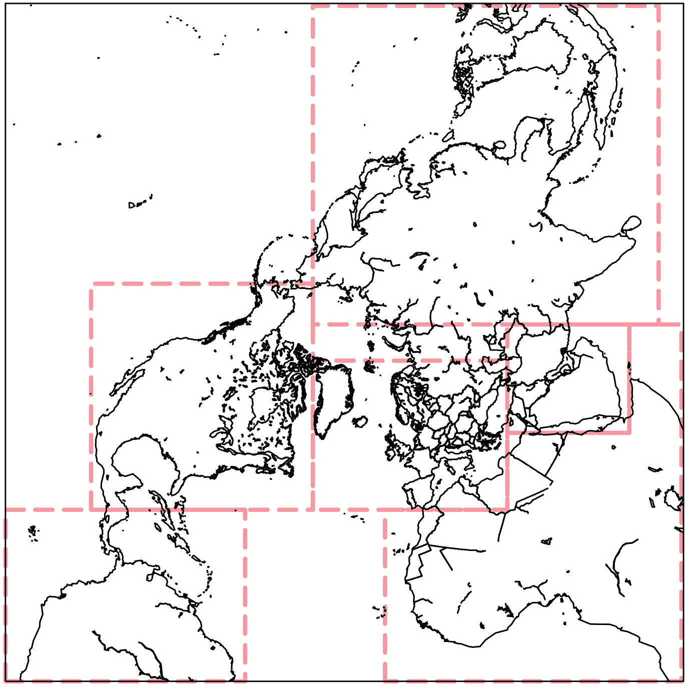

Fig. 15. The DEHM mother domain used in this study which covering more than the Northern Hemisphere, together with six regions; North America, South America, Asia, Europe, Middle East and Africa. Total contributions from individual natural source category to O_3 and $PM_{2.5}$level over the six regions are calculated.

ACPD
13, 16775–16830, 2013

CC BY